

Summary of the project

FEATURE EXTRACTION OF EARTHQUAKE SIGNALS USING FRACTIONAL DOMAIN

ORIGIN OF THE RESEARCH PROBLEM:

Earlier methods are used to analyse the feature extraction of Earthquake signals by Fourier transform (FT), Short Time Fourier Transform (STFT), Continuous Wavelet Transform (CWT)[3] are fixed with respect to their kernel function but, implementation of feature extraction[2] with Fractional Fourier Transform (FrFT) or combinations of different transforms with various windows combinations will give a better input to the pattern matching in terms of their spectral quality of the Earthquake signals. Recently in literature, FrFT plays significant role in signal processing [4]. It is generalization Fourier transforms, whose kernel functions gives better resolutions in terms of spectral analysis of signals by virtue of its kernel function. Necessary filters will be implement in FrFT domain, In fact it helps to analyse better identification of Earthquake.

SIGNIFICANCE OF THE STUDY:

The Vulnerability of human civilization to disasters caused by large earthquake is growing due to the clustering of populations and proliferation of high-risk objects. The disasters have become a threat to a civilization's well-being today a single earthquake may take up to several hundred thousand lives and cause significant material damage. The problem of earthquake prediction is a grand challenge although it may be solvable [6].

Objectives:

The main objective of the project is to extract the feature of SES using FrFT or combination of different transforms in order to improve the accuracy in detecting earthquake.

Objective tasks are to be performed

1. Study of Seismic Electrical Signal (SES).
2. Investigation of existing feature extraction methods and pattern matching methods.
3. Implementation of window function either with FrFT or possible combination of different transform. All possible filters will be implemented in the FrFT domain.

Comparison of Butterworth & Novel Butterworth filter:

Butter worth filter	Novel Butter worth filter
<ul style="list-style-type: none"> The Butter worth filter equation is given by, $H(j\Omega) = \frac{1}{\sqrt{\left(1 + \left(\frac{\Omega}{\Omega_c}\right)^{2N}\right)}}$ <p style="text-align: center;">Where Ω = variable frequency, Ω_c=cut-off frequency, N= order.</p> <ul style="list-style-type: none"> For specific order. Flat response in pass band Cut-off frequencies are easily find out due to flat response. No ripples in transition band 	<ul style="list-style-type: none"> The Novel Butter worth filter equation is given by, $H(j\Omega) = \frac{1}{\sqrt{\left(1 + \left(\frac{\exp\left(\frac{\Omega}{\Omega_c}\right)}{2.71828}\right)^{2N}\right)}}$ <p style="text-align: center;">Where Ω = variable frequency, Ω_c=cut-off frequency, N= order.</p> <ul style="list-style-type: none"> Order decreases. More flat response compared to butter worth Cut-off frequencies are accurately find out due to more flat response. No ripples in transition band

The Table , gives the major comparisons of the two Butterworth Filters.

CONCLUSION:

It is concluded that the new featured Butterworth filter gives better lower order for given specification than the existing filter .It is also gives better spectral characteristics than existing Butterworth window that too better than the Dirichlett ,Triangle window functions.

Also the Signal to Noise Ratio which is calculated earlier is increased than usual, when compared between Conventional Butterworth Filter, Modified Butterworth Filter and Fractional Modified Butterworth Filter as mentioned in the previous chapter.

Thus our project successfully explains that the order of the filter gets reduced and the use of our Novel Butterworth Filter in the analysis of Earthquake Signals. The future scope of this project can be implemented using the FIR window techniques and predicting the Earthquake signals.

1.1 INTRODUCTION

Earthquake is one of the natural disasters that results in major distraction. Many efforts have been put in place in order to reduce disastrous effect of earthquake[1]. Seismic waves can be categorized into two types[2]. The categorization is based upon the way the seismic waves travel through the medium. Note that the enumeration of seismic wave types is not complete but the most important types are given[2]. The first types of seismic waves are referred to as body waves. The second types of waves are called surface waves. Body waves can travel through the earth inner layers, whereas surface waves like name already suggest can only travel through the earth surface.

Earthquakes usually radiate both body and surface wave. Surface waves are almost always responsible for most of the damage in the event of an earthquake. Because surface waves can only travel along the earth surface the energy of surface waves is reduced for deeper earthquake[2].

There are two important stages in the Earthquake prediction, one is feature extraction and other is pattern matching.

Feature extraction is a process of extracting the first significant change of Seismic Electrical Signal (SES) used to represent SES.

The second process is pattern matching is a process of identification of the earthquake prediction information, namely time, magnitude, and epicentre of the incoming earthquake.

Many methods were proposed for feature extraction of Earthquake signals such as wavelet, short time Fourier transform, Fourier transform adaptive short time Fourier transforms.

Since feature extraction technique of the first significant change of the SES is used as input to the pattern matching process. So that, identification of Earthquake is possible.

1.2 MOTIVATION

• ORIGIN OF THE RESEARCH PROBLEM:

Earlier methods are used to analyse the feature extraction of Earthquake signals by Fourier transform (FT), Short Time Fourier Transform (STFT), Continuous Wavelet Transform (CWT)[3] are fixed with respect to their kernel function but, implementation of feature extraction[2] with Fractional Fourier Transform (FrFT) or combinations of different transforms with various windows combinations will give a better input to the pattern matching in terms of their spectral quality of the Earthquake signals. Recently in literature, FrFT plays significant role in signal processing [4]. It is generalization Fourier transforms, whose kernel functions gives better resolutions in terms of spectral analysis of signals by virtue of its kernel function. Necessary filters will be implement in FrFT domain, In fact it helps to analyse better identification of Earthquake.

• SIGNIFICANCE OF THE STUDY:

The Vulnerability of human civilization to disasters caused by large earthquake is growing due to the clustering of populations and proliferation of high-risk objects. The disasters have become a threat to a civilization's well-being today a single earthquake may take up to several hundred thousand lives and cause significant material damage. The problem of earthquake prediction is a grand challenge although it may be solvable [6].

1.3 Objectives:

The main objective of the project is to extract the feature of SES using FrFT or combination of different transforms in order to improve the accuracy in detecting earthquake.

Objective tasks are to be performed

1. Study of Seismic Electrical Signal (SES).

FEATURE EXTRACTION OF EARTHQUAKE SIGNALS USING FRACTIONAL DOMAIN

2. Investigation of existing feature extraction methods and pattern matching methods.

3. Implementation of window function either with FrFT or possible combination of different transform. All possible filters will be implemented in the FrFT domain.

2.1 INTRODUCTION TO EARTHQUAKE

An earthquake (also known as a quake, tremor or temblor) is the perceptible shaking of the surface of the Earth, resulting from the sudden release of energy in the Earth's crust that creates seismic waves.

Earthquakes can be violent enough to toss people around and destroy whole cities. The seismicity or seismic activity of an area refers to the frequency, type and size of earthquakes experienced over a period of time. Earthquakes are measured using observations from seismometers [2]. The moment magnitude is the most common scale on which earthquakes larger than approximately 5 are reported for the entire globe. The more numerous earthquakes smaller than magnitude 5 reported by national seismological observatories are measured mostly on the local magnitude scale, also referred to as the Richter magnitude scale.

In its most general sense, the word *earthquake* is used to describe any seismic event — whether natural or caused by humans — that generates seismic waves. Earthquakes are caused mostly by rupture of geological faults, but also by other events such as volcanic activity, landslides, mine blasts, and nuclear tests. An earthquake's point of initial rupture is called its focus or hypocenter. The epicenter is the point at ground level directly above the hypocenter

Tectonic earthquakes occur anywhere in the earth where there is sufficient stored elastic strain energy to drive fract propagation along a fault planeure. The sides of a fault move past each other smoothly and aseismically only if there are no irregularities or asperities along the fault surface that increase the frictional resistance [2]. Most fault surfaces do have such asperities and this leads to a form of stick-slip behavior. Once the fault has locked, continued relative motion between the plates leads to increasing stress and therefore, stored strain energy in the volume around the fault surface. This continues until the stress has risen sufficiently to break through the asperity, suddenly allowing sliding over the locked portion of the fault, releasing the stored energy. This energy is released as a combination of radiated elastic strain seismic waves, frictional heating of the

fault surface, and cracking of the rock, thus causing an earthquake. This process of gradual build-up of strain and stress punctuated by occasional sudden earthquake failure is referred to as the elastic-rebound theory.

Earthquake fault types

There are three main types of fault, all of which may cause an interplate earthquake: normal, reverse (thrust) and strike-slip. Normal faults occur mainly in areas where the crust is being extended such as a divergent boundary [10]. Reverse faults occur in areas where the crust is being shortened such as at a convergent boundary. Strike-slip faults are steep structures where the two sides of the fault slip horizontally past each other; transform boundaries are a particular type of strike-slip fault.

Earthquakes and volcanic activity

Earthquakes often occur in volcanic regions and are caused there, both by tectonic faults and the movement of magma in volcanoes. Such earthquakes can serve as an early warning of volcanic eruptions, as during the Mount St. Helens eruption of 1980.^[18] Earthquake swarms can serve as markers for the location of the flowing magma throughout the volcanoes. These swarms can be recorded by seismometers and tilt meters (a device that measures ground slope) and used as sensors to predict imminent or upcoming eruptions.

Rupture dynamics

A tectonic earthquake begins by an initial rupture at a point on the fault surface, a process known as nucleation. The scale of the nucleation zone is uncertain, with some evidence, such as the rupture dimensions of the smallest earthquakes, suggesting that it is smaller than 100 m while other evidence, such as a slow component revealed by low-frequency spectra of some earthquakes, suggests that it is larger. The possibility that the nucleation involves some sort of preparation process is supported by the observation that about 40% of earthquakes are preceded by foreshocks. Once the rupture has initiated, it begins to propagate along the fault surface. The mechanics of this process are poorly understood, partly because it is difficult to recreate the high sliding velocities in a laboratory.

Also the effects of strong ground motion make it very difficult to record information close to a nucleation zone.

Rupture propagation is generally modeled using a fracture mechanics approach, likening the rupture to a propagating mixed mode shear crack. The rupture velocity is a function of the fracture energy in the volume around the crack tip, increasing with decreasing fracture energy. The velocity of rupture propagation is orders of magnitude faster than the displacement velocity across the fault. Earthquake ruptures typically propagate at velocities that are in the range 70–90% of the S-wave velocity, and this is independent of earthquake size. A small subset of earthquake ruptures appear to have propagated at speeds greater than the S-wave velocity. These super shear earthquakes have all been observed during large strike-slip events. The unusually wide zone of co seismic damage caused by the 2001 Kunlun earthquake has been attributed to the effects of the sonic boom developed in such earthquakes. Some earthquake ruptures travel at unusually low velocities and are referred to as slow earthquakes. A particularly dangerous form of slow earthquake is the tsunami earthquake, observed where the relatively low felt intensities, caused by the slow propagation speed of some great earthquakes, fail to alert the population of the neighboring coast, as in the 1896 Meiji-Sanriku earthquake.

Earthquake clusters

Most earthquakes form part of a sequence, related to each other in terms of location and time. Most earthquake clusters consist of small tremors that cause little to no damage, but there is a theory that earthquakes can recur in a regular pattern. An aftershock is an earthquake that occurs after a previous earthquake, the main shock. An aftershock is in the same region of the main shock but always of a smaller magnitude

Aftershocks

An aftershock is an earthquake that occurs after a previous earthquake, the main shock. An aftershock is in the same region of the main shock but always of a

smaller magnitude[10]. If an aftershock is larger than the main shock, the aftershock is redesignated as the main shock and the original main shock is redesignated as a foreshock. Aftershocks are formed as the crust around the displaced fault plane adjusts to the effects of the main shock.

Earthquake swarms

Earthquake swarms are sequences of earthquakes striking in a specific area within a short period of time. They are different from earthquakes followed by a series of aftershocks by the fact that no single earthquake in the sequence is obviously the main shock, therefore none have notable higher magnitudes than the other. An example of an earthquake swarm is the 2004 activity at Park. In August 2012, a swarm of earthquakes shook Southern California's Imperial Valley, showing the most recorded activity in the area since the 1970s.

Earthquake storm

Sometimes a series of earthquakes occur in a sort of earthquake storm, where the earthquakes strike a fault in clusters, each triggered by the shaking or stress redistribution of the previous earthquakes. Similar to aftershocks but on adjacent segments of fault, these storms occur over the course of years, and with some of the later earthquakes as damaging as the early ones. Such a pattern was observed in the sequence of about a dozen earthquakes that struck the North Anatolian Fault in Turkey in the 20th century and has been inferred for older anomalous clusters of large earthquakes in the Middle East.

Earthquake is one of the most destructive of natural disasters that killed many people and destroyed a lot of properties. Earth's electric field is one of the features that can be used to predict earthquakes (EQs). The Feature Extraction method is the best technique to analyze earthquake which is explained in detail later on.

2.2 FEATURE EXTRACTION OF EARTHQUAKE

Earthquake is one of the most destructive of natural disasters that killed many people and destroyed a lot of properties. By considering these catastrophic effects,

it is highly important of knowing ahead of earthquakes in order to reduce the number of victims and material losses. Earth's electric field is one of the features that can be used to predict earthquakes (EQs), since it has significant changes in the amplitude of the signal prior to the earthquake

In machine learning, pattern recognition and in image processing, **feature extraction** starts from an initial set of measured data and builds derived values (features) intended to be informative and non-redundant, facilitating the subsequent learning and generalization steps, and in some cases leading to better human interpretations. Feature extraction is related to dimensionality reduction.

When the input data to an algorithm is too large to be processed and it is suspected to be redundant (e.g. the same measurement in both feet and meters, or the repetitiveness of images presented as pixels), then it can be transformed into a reduced set of features (also named a features vector). This process is called *feature extraction*. The extracted features are expected to contain the relevant information from the input data, so that the desired task can be performed by using this reduced representation instead of the complete initial data.

Feature extraction involves reducing the amount of resources required to describe a large set of data. When performing analysis of complex data one of the major problems stems from the number of variables involved. Analysis with a large number of variables generally requires a large amount of memory and computation power, also it may cause a classification algorithm to over fit to training samples and generalize poorly to new samples. Feature extraction is a general term for methods of constructing combinations of the variables to get around these problems while still describing the data with sufficient accuracy.

The best results are achieved when an expert constructs a set of application-dependent features, a process called feature engineering. Nevertheless, if no such expert knowledge is available, general dimensionality reduction techniques may help. These include:

- Principal component analysis
- Semi definite embedding
- Multifactor dimensionality reduction
- Multilinear subspace learning
- Nonlinear dimensionality reduction
- Isomap
- Kernel PCA
- Multilinear PCA
- Latent semantic analysis
- Partial least squares
- Independent component analysis
- Auto encoder

The feature extraction technique plays a predominant role in Image Processing. This Feature can also be used in the Earthquake Prediction. An event called prediction in a time series is more important for geophysics and economy problems. The time series data mining is a combination field of time series and data mining techniques. The historical data are collected which has follow the time series methodology, combine the data mining for preprocessing and finally apply the fuzzy logic rules to predict the impact of earthquake.

Earthquake prediction has done by historical earthquake time series to investigating the method at first step ago. Huge data sets are preprocessed using data mining techniques. Based on this process data prediction is possible. This paper is focused on statistics and soft computing techniques to analyze the earthquake data.

2.2.1 INTRODUCTION:

A time series includes a huge number of observations are well defined data items ordered in equal time or equal space. The collected data are irregular or happens only once are not a time series data. An observed time series are categorized into three types as follows:

1. The Seasonal component
2. The Trend component and
3. The Irregular component.

The seasonal data are systematic or regular movements of data. The Trend data mean by Long-term fluctuations and the irregular data mean by unsystematic or short-term fluctuations. The major utility area of the time series model is statistical forecasting. The available prediction approaches are regression, time series and chaotic approaches. Each and every method has its own advantage and disadvantage.

The historical sequences of data are to be used for forecasting purposes, because of this reason the time series models are used to predict the future values. The prediction will show what will happen but won't why it happens. Time series values are transformed to phase space by using a nonlinear method and then apply the fuzzy logic to predict optimum value. The time series data are derived from the time interval of any system. Traditional stationary time series models are Autoregressive Integrated Moving Average (ARIMA) and Minimum Mean Square Error forecasting methods.

Data mining is used to extract useful and more relevant information from the huge database. The author Han describes an artificial intelligence and pattern recognition methods for prediction. The time series data mining is used for prediction of earthquake [5]. Fuzzy logic methods are used to predict the earthquake, stock market changes, weather forecasting and gold price changes. The similarities of patterns are selected as a fuzzy set; these sets are specified in

membership function. The fuzzy logic is accurately predicted the prediction event. The concepts of time series data mining had been used for clustering and natural event prediction. Povinelli, suggested an application for the event prediction.

In their study, they focus the different applications such as earthquake prediction, fall of stock price and gold price prediction. The major advantage of time series is possible to predict the future value based on the previous historical data. The study of the past sequence of historical data may be more valuable. The time series is helpful to predict the next sequence of future values. The utility of time series method is specifically for Trend analysis, Trade market, finance, Climatologic and earthquake prediction.

2.3 EXISTING FILTERS OF EARTHQUAKE

An ideal filter is a network that allows signals of only certain frequencies to pass while blocking all others. Depending on the regime of frequencies that are allowed through or not they are characterized as low-pass, high-pass, band-pass, band-reject and all-pass [2] [5]. There are many needs for electric filters, some of the more common being those used in radio and television sets, which allow tuning in a certain channel by passing its band of frequencies while filtering out those of other channels. The frequency response is divided into magnitude (amplitude) and phase parts. The amplitude curve of a filter will indicate how closely the practical circuit imitates the ideal filter characteristics that are as follows:

1. Low pass filter,
2. High pass filter,
3. Band pass filter,
4. Band reject filter.
5. All pass filter.

Notice that, depending on the relative magnitude of their corner frequencies, a low pass in series with a high pass can either completely block all signals or give a band reject. By the same token, a low pass in parallel with a high pass can give either a bandpass or an all pass.

These ideal characteristics will at best be approximated by real circuits. How closely this will be achieved will depend on the frequency response of the particular circuit. The design of electric filters is based on a compromise between deviation from ideality vs. complexity (and cost)[6]. The order of the polynomial being used (thus the order of the filter) is the major indicator: the higher the order, the more complex the circuit and the closer the frequency response to the ideal curve. Filter operation is considered when the amplitude of the output signal of the circuit is relatively large for some frequencies and small for others. Then one can say that for the former the signal passes and for the latter it does not.

1. Low pass filter:

The magnitude response of the ideal low pass filter allows the low frequencies in the pass band $0 < \Omega < \Omega_c$ to pass, whereas the higher frequencies in the stop band $\Omega > \Omega_c$ are blocked as shown in Figure 2.1. The frequency Ω_c between the two bands is cutoff frequency, where the magnitude $|H(j\Omega)| = 1/\sqrt{2}$.

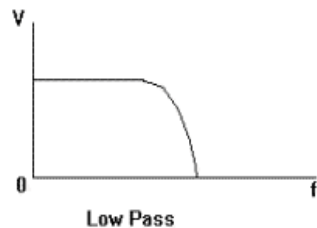


Figure 2.1: Response of LOW-PASS FILTER

2. High pass filter:

The high pass filter allows high frequencies above $\Omega > \Omega_c$ and rejects the frequencies between $\Omega = 0$ and $\Omega = \Omega_c$ as shown in Figure 2.2. The magnitude response of a high pass filter is shown in figure.

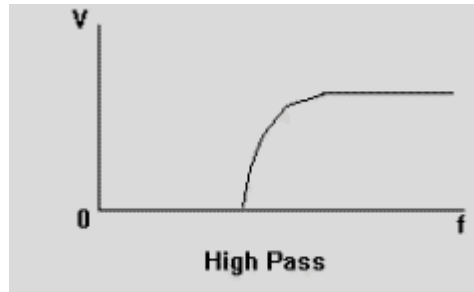


Figure2.2: Response of HIGH-PASS FILTER

3. Band pass filter:

It allows only a band frequencies Ω_1 to Ω_2 to pass and stop all other frequencies as shown in Figure 2.3. The practical response of band pass filter is shown in figure.

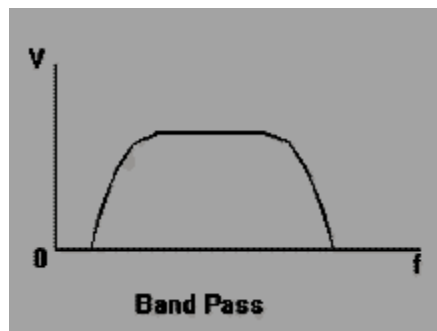


Figure 2.3:Response of BAND-PASS FILTER

4. Band reject filter:

It rejects all the frequencies between Ω and Ω and allows remaining frequencies. The magnitude response of practical band reject filter is shown in Figure 2.4.

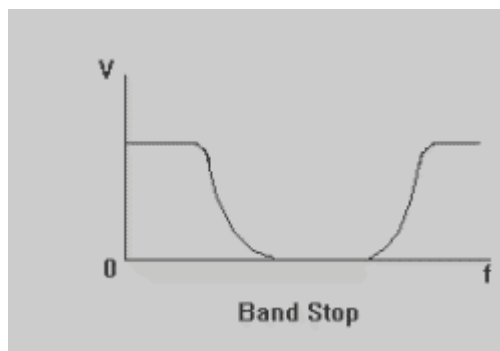


Figure 2.4: Response of BAND-STOP FILTER

5. All pass filter:

An all-pass filter is defined as a system which has a constant magnitude response at all frequencies. Pure delay system is an example of this type of filter.

2.3.1 ANALOG FILTERS

- Analog filter is a system in which both the input and the output are continuous-time signals.
- Implementation of these filters is carried out using passive components (resistors, capacitors, inductors) and active components (transistors, operational amplifiers).
- These operate in infinite frequency range[7].
- These have frequency range of operation as well as they can interact directly with the analog world.
- Main disadvantages of analog filters are its higher noise sensitivity, non-linearity, dynamic range limitations, lack of flexibility in designing and reproductivity, errors generated due to drift and variations in the value of active and passive components used in the circuits.

2.3.2 DIGITAL FILTER

- Digital filter is a system in which both the input and output are discrete time signals.
- These are implemented on a digital computer or micro computer using DSP integrated circuits.
- Frequency range is restricted to half of the sampling rate.
- These filters require additional A/D and D/A converter sections for connecting to the physical analog world.
- Main advantages of the digital filters are that these are insensitive to noise, higher linearity, unlimited dynamic range, flexibility in software design, high accuracy and reliability is higher.

2.3.3 Design of Digital filters from Analog filters:

The most common technique used for designing IIR digital filters known as indirect method, involves first designing an analog prototype filter and then transforming the prototype to a digital filter[8]. For the given specifications of a digital filter, the derivation of the digital filter transfer function requires three steps.

1. Map the desired digital filter specifications into those for an equivalent analog filter.
2. Derive the analog transfer function for the analog prototype.
3. Transform the transfer function of the analog prototype into an equivalent digital filter transfer function.

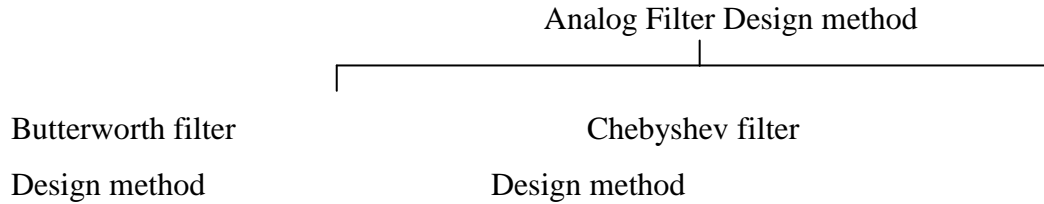
2.3.4 Advantages of Digital Filter:

- Unlike analog filters, the digital filter performance is not influenced by component ageing, temperature and power supply variations.
- These are highly immune to rise and possess considerable parameter stability.
- Digital filters afford a wide variety of shapes for amplitude and phase response.
- There are no problems of input and output impedance matching with digital filters [9].
- These can be operated over a wide range of frequencies.
- The coefficients of digital filters can be programmed and altered any time to obtain the desired characteristics [10].
- Multiple filtering is possible only in digital filters.

2.3.5 Disadvantages:

- The quantization error arises due to finite-word length in the representation of signal and parameter.

2.3.6 Filter Design methods:



2.3.7 Butter worth filter design method:

Transfer Function:

$$|N(j\Omega)| = \frac{1}{\left[1 + \left(\frac{\Omega}{\Omega_c}\right)^{2N}\right]^{1/2}}; \quad N = 1, 2, 3, \dots$$

As ‘N’ order of the filter increases [13], the filter response approaches Ideality. As shown in fig.

$$|N(j\Omega)|^2 = \frac{1}{1 + (\Omega)^{2N}} \quad \text{where } \Omega_c = 1 \text{ rad/sec}$$

i.e., normalized

$$|N(j\Omega)|^2 = N(\Omega)^2 \quad \text{we know that } \Omega = \delta/j$$

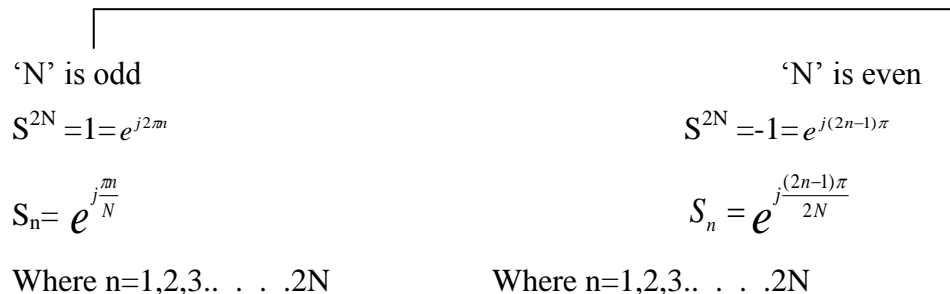
$$|N(j\Omega)|^2 = N(-\delta^2) = N(\delta)M(-\delta)$$

$$N(\delta)M(-\delta) = \frac{1}{1 + \left(\frac{\delta}{j}\right)^{2N}} = \frac{1}{1 + (-1)^{N,2N}} = \frac{1}{1 + (-\delta^2)^N}$$

To find the roots, characteristic equation

should be equal of zero

$$\text{i.e., } 1 + (-\delta^2)^N$$



2.3.8.1 List of Butter worth polynomials[13]:

N

Denominator of N(s)

1	$S+1$
2	$S^2+\sqrt{2}S+1$
3	$(S+1)(S^2+S+1)$
4	$(S^2+0.76537S+1)(S^2+1.8477S+1)$
5	$(S+1)(S^2+0.6180S+1)(S^2+1.618S+1)$
6	$(S^2+1.931S+1)(S^2+\sqrt{2}S+1)(S^2+0.51764S+1)$

Transfer function of the above table are normalized equations with $\Omega_c = 1 \text{ rad/s}$.

The transfer function of Butter worth filter can be obtained by

$$S \leftarrow \frac{S}{\Omega_c}$$

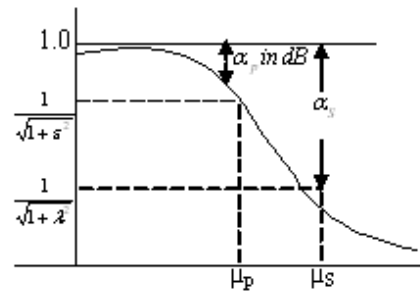
2.3.8.2 Designing LPF Butter worth Filter:

$$N(j\Omega) = \frac{1}{\left[1 + \varepsilon^2 \left(\frac{\Omega}{\Omega\rho}\right)^{2N}\right]^{1/2}}$$

$$|N(j\Omega)|^2 = \frac{1}{\left[1 + \varepsilon^2 \left(\frac{\Omega}{\Omega\rho}\right)^{2N}\right]}$$

Apply '10 log' both sides

$$20 \log [N(j\Omega)] = 10 \log (1) - 10 \log \left[1 + \varepsilon^2 \left(\frac{\Omega}{\Omega\rho}\right)^{2N}\right]$$



At $\Omega = \Omega\rho$ the attenuation equal to ' α_p '

So,

$$20 \log [N(j\Omega)] = -\alpha_\rho = -10 \log (1 + \varepsilon^2)$$

$$0.1 \alpha_\rho = \log (1 + \varepsilon^2)$$

$$\varepsilon^2 = 10^{0.1 \alpha_\rho} - 1$$

$$\varepsilon = (10^{0.1 \alpha_\rho} - 1)^{1/2}$$

At $\Omega = \Omega_s$, the attenuation is ' α_s '

$$20 \log [N(j\Omega)] = -\Omega_\rho = -10 \log \left(1 + \varepsilon^2 \left(\frac{\Omega}{\Omega_\rho} \right)^{2N} \right)$$

$$\left(1 + \varepsilon^2 \left(\frac{\Omega}{\Omega_\rho} \right)^{2N} \right) = 10^{0.1 \alpha_s}$$

$$\varepsilon^2 \left(\frac{\Omega}{\Omega_\rho} \right)^{2N} = 10^{0.1 \alpha_s} - 1$$

$$(10^{0.1 \alpha_\rho} - 1) \left(\frac{\Omega_s}{\Omega_\rho} \right)^{2N} = 10^{0.1 \alpha_s} - 1$$

$$\left(\frac{\Omega_s}{\Omega_\rho} \right)^{2N} = \frac{10^{0.1 \alpha_s} - 1}{10^{0.1 \alpha_\rho} - 1}$$

$$\left(\frac{\Omega_s}{\Omega_\rho} \right)^{2N} = \sqrt{\frac{10^{0.1 \alpha_s} - 1}{10^{0.1 \alpha_\rho} - 1}}$$

$$\left(\frac{\Omega_s}{\Omega_\rho} \right)^{2N} = \sqrt{\frac{10^{0.1 \alpha_s} - 1}{10^{0.1 \alpha_\rho} - 1}}$$

$$N \log \left(\frac{\Omega_s}{\Omega_\rho} \right)^{2N} = \log \sqrt{\frac{10^{0.1\alpha_s} - 1}{10^{0.1\alpha_\rho} - 1}}$$

$$N \geq \frac{\log \sqrt{\frac{10^{0.1\alpha_s} - 1}{10^{0.1\alpha_\rho} - 1}}}{\log \left(\frac{\Omega_s}{\Omega_\rho} \right)^{2N}}$$

$$N \geq \frac{\log \sqrt{\frac{\lambda}{\varepsilon}}}{\log \left(\frac{\Omega_s}{\Omega_\rho} \right)^{2N}}$$

where $\lambda = \sqrt{(10^{0.1\alpha_s} - 1)}$

$\varepsilon = \sqrt{(10^{0.1\alpha_\rho} - 1)}$

Problem 1: Given specification $\alpha_\rho=1\text{dB}$, $\alpha_s=30\text{dB}$; $\Omega_\rho = \text{rad}/s$; $\Omega_s=600 \text{ rad/sec}$;

determine [13] $N=?$

Ans:

$$\sqrt{\frac{\lambda}{\varepsilon}} = \sqrt{\frac{10^{0.1\alpha_s} - 1}{10^{0.1\alpha_\rho} - 1}} = \sqrt{\frac{10^3 - 1}{10^{0.1} - 1}} = 62.115$$

$$\frac{\Omega_s}{\Omega_\rho} = 3$$

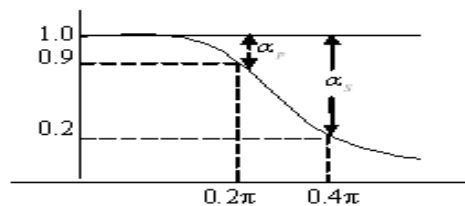
$$\frac{\Omega_s}{\Omega_\rho} = \frac{\log(62.115)}{\log(3)} = 3.758$$

$$N = 4$$

Problem 2: For given specification design an analog butter worth filter $0.9 <$

$N(j\Omega) < 1$ for $0 < \Omega < 0.2\pi$; $N(j\Omega) < 0.2$ for $0.4\pi < \Omega < \pi$

Ans: from given data



$$\Omega_\rho = 0.2\pi; \Omega_s = 0.4\pi$$

$$\frac{1}{\sqrt{1+\varepsilon^2}} = 0.9 \quad \& \quad \frac{1}{\sqrt{1+\varepsilon^2}} = 0.2$$

$$\varepsilon = 0.484 \quad \& \quad \lambda = 4.898$$

$$N \geq \frac{\log\left(\frac{\lambda}{\varepsilon}\right)}{\log\left(\frac{\Omega_s}{\Omega_\rho}\right)}$$

$$N = 4$$

$$\Omega_c = \frac{\Omega_\rho}{(\varepsilon)^{\frac{1}{N}}} = 0.24\pi$$

$$S \leftarrow \frac{S}{0.24\pi}$$

$$\text{Hence } H(s) = \frac{0.323}{(S^2 + 0.577S + 0.0576\pi^2)(S^2 + 1.393S + 0.0576\pi^2)}$$

2.3.8.3 IIR (INFINITE IMPULSE RESPONSE) DIGITAL FILTERS:

- Impulse response of these digital filters are computed for infinite number of samples and hence called Infinite Impulse Response filters.

$$H(n) \neq 0, \quad 0 \leq n \leq \infty$$

- These filters are characterized by the rational system function as

$$H(Z) = \frac{\sum_{K=0}^M B_K Z^{-K}}{1 + \sum_{K=0}^N A_K Z^{-K}}$$

- The present output of these filters depends on the previous outputs as well as present and past inputs.

- These filters do not have linear phase and these are generally used where some phase distortion is tolerable[12].
- Theoretically these filters are stable but after truncating their coefficients these become unstable and these have less flexibility for obtaining non-standard frequency responses are for those filters for which analog filter design techniques are not available.
- There are shorter time delays in these filters.
- These require lesser number of arithmetic operations and these have lower computational complexity and smaller memory requirements.
- IIR filters have resemblance with analog filters.

2.3.8.4 Design of IIR Filter form analog Filter:

There are several methods that can be used to design digital filters having an infinite duration unit sample response. The techniques describes here are all based on converting an analog filter into a digital filter[14]. For the conversion technique to be effective, it should process the following desirable properties:-

1. The $j\omega$ -axis in the s-plane should map into the unit circle in the Z-plane. Thus there will be a direct relationship between the two frequency variables in the two domains.
2. The left half of the s-plane should map into the inside of the unit circle in the Z-plane, thus a stable analog filter will be converted to a stable digital filter.

The corresponding discrete-time transfer function $H_d(Z)$ of an IIR digital filter is obtained from continuous transfer function $H_a(S)$ of an analog filter. The approximation is obtained using one of the following methods:

- Approximation of derivatives
- Impulse Response Invariance method
- The matched Z-transform
- Bilinear transformation method

2.3.8.4 Impulse invariance method:In this method, IIR filter is designed such that the unit impulse response $h(n)$ of digital filter is the sampled version of the impulse response of analog filter[15].

Z-transform of an infinite impulse response is by

$$H(z) = \sum_{n=0}^{\infty} h(n)z^{-n}$$

$$H(z)\Big|_{z=e^{sT}} = \sum_{n=0}^{\infty} h(n)e^{-sTn}$$

$$Z = e^{sT}$$

$$re^{j\omega} = e^{(\sigma + j\Omega)T}$$

$$re^{j\omega} = e^{\sigma T} e^{j\Omega T}$$

$$\text{so } r = e^{\sigma T} \ \& \ \omega = \Omega T$$

Thus pole in S-plane mapped into Z-plane the real value decides the magnitude i.e., $e^{\sigma T}$

The imaginary value decides an angle i.e., $\omega = \Omega T$ as shown in Figure 2.5.

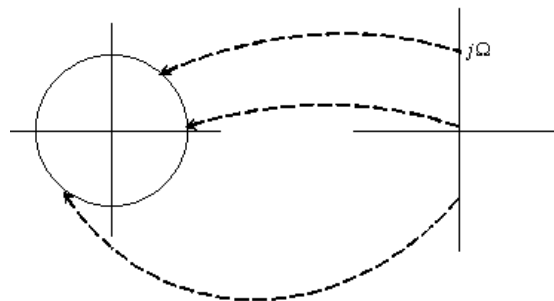


Figure 2.5

Corresponding mathematics for

- (a) **Stability:**- $r = e^{\sigma T} < 1$ for $\sigma < 0$ in it all poles map inside the unit circle.
- (b) **Unstable:**- $r = e^{\sigma T} > 1$ for $\sigma > 0$ in it all poles map outside the unit circle

Disadvantages:

Mapping many to one:

$$S_1 = \sigma + j\Omega$$

$$S_2 = \sigma + j\left(\Omega + \frac{2\pi}{T}\right)$$

$$Z_1 = e^{S_1 T} = e^{\sigma T} \cdot e^{j\Omega T}$$

$$\begin{aligned} Z_2 &= e^{S_2 T} = e^{\sigma T} \cdot e^{j\left(\Omega T + \frac{2\pi}{T} T\right)} \\ &= e^{\sigma T} \cdot e^{j\Omega T} \cdot e^{j2\pi} \end{aligned}$$

$$= e^{\sigma T} \cdot e^{j\Omega T} \quad \left[\because e^{j2\pi} = 1 \right]$$

Z₁, and Z₂ are equal

Thus aliasing occur

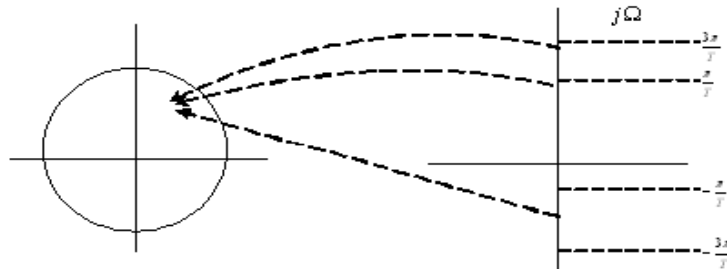


Figure 2.6

All poles in $j\Omega$ –Plane map at same location in Z-plane. Thus S-plane having imaginary parts greater than $\frac{\pi}{T}$ or less than $-\frac{\pi}{T}$ case aliasing, when sampling analog signal as shown in Figure 2.6.

Conversion:

Let $H_a(S)$ is Analog transfer function $H_a(s) = \sum_{k=1}^N \frac{C_k}{S - p_k}$

Apply inverse Laplace

$$h_a(z) = \sum_{k=1}^N C_k e^{p_k t} \quad \text{for } t \geq 0$$

If we sample $h_a(t)$ periodically

$$T = nT$$

$$H(n) = h_a(nT)$$

$$\begin{aligned} h(n) &= \sum_{k=1}^N C_k e^{p_k nT} \\ H(z) &= \sum_{n=0}^{\infty} \sum_{k=1}^N C_k e^{p_k nT} z^{-n} \\ &= \sum_{k=1}^N C_k \sum_{n=0}^{\infty} [e^{p_k T} z^{-1}]^n \\ &= \sum_{k=1}^N \frac{C_k}{1 - e^{p_k T} z^{-1}} \end{aligned}$$

for sampling rates

$$= \sum_{k=1}^N \frac{TC_k}{1 - e^{p_k T} z^{-1}}$$

Problem 5 $H(s) = \frac{2}{(S+1)(S+2)}$ determine $H(z)$ using impulse invariance.

Assume $T=1$ sec.

Ans:-

$$\begin{aligned} H(s) &= \frac{2}{(S+1)(S+2)} \\ H(s) &= \frac{2}{S - (-1)} - \frac{2}{S - (-2)} \\ P_1 &= -1; \quad P_2 = -2 \\ &= \frac{(T)(2)}{1 - e^{-T} z^{-1}} - \frac{(T)(2)}{1 - e^{-2T} z^{-1}} \\ &= \frac{2}{1 - e^{-T} z^{-1}} - \frac{2}{1 - e^{-2} z^{-1}} \\ &= \frac{0.465z^{-1}}{1 - 0.503z^{-1} + 0.04976z^{-2}} \end{aligned}$$

2.3.8.5 Bilinear Transfer Function:

$$\text{Let } H(s) = \frac{b}{S+a}$$

$$\frac{y(s)}{x(s)} = \frac{b}{S+a}$$

$$Sy(s) + a y(s) = b x(s)$$

This can be characterized by differential equation

$$\frac{dy(t)}{dt} + a y(t) = b x(t)$$

$y(t)$ can be approximately as Trapezoidal formula

$$y(t) = \int_{t_0}^t y^1(\tau) d\tau + y(t_0)$$

$$t = nT; \quad t_0 = nT - T \quad \text{yields}$$

$$y(nT) = \frac{T}{2} [y^1(nT) + y^1(nT - T)] + y^1(nT - T)$$

$$S = \frac{2}{T} \left[\frac{1 - z^{-1}}{1 + z^{-1}} \right] \Rightarrow \frac{2}{T} \left(\frac{z - 1}{z + 1} \right)$$

$$z = r e^{j\omega}$$

$$S = \frac{2}{T} \left[\frac{r e^{j\omega} - 1}{r e^{j\omega} + 1} \right] = \frac{2}{T} \left[\frac{r \cos \omega - 1 + j r \sin \omega}{r \cos \omega + 1 + j r \sin \omega} \right]$$

$$S = \frac{2}{T} \left[\frac{r^2 - 1}{1 + r^2 + 2r \cos \omega} + j \frac{2r \sin \omega}{1 + r^2 + 2r \cos \omega} \right]$$

$$\therefore \sigma = \frac{2}{T} \left[\frac{r^2 - 1}{1 + r^2 + 2r \cos \omega} \right]$$

$$\Omega = \frac{2}{T} \left[\frac{2r \sin \omega}{1 + r^2 + 2r \cos \omega} \right]$$

If $r < 1$ then $\sigma < 0$

If $r > 1$ then $\sigma > 0$

So, LHP of 'S' maps inside the unit circle

RHP of 'S' maps outside the unit circle

$r = 1$ then $\sigma = 0$

$$\Omega = \frac{2 \sin \omega}{T(1 + \cos \omega)} \Rightarrow \frac{2}{T} \tan \frac{\omega}{2}$$

$$\text{Hence } \omega = 2 \tan^{-1} \left(\frac{\Omega T}{2} \right)$$

small values of ' ω '

$$\Omega = \frac{2}{T} \left(\frac{\omega}{2} \right)$$

$$\Omega = \left(\frac{\omega}{T} \right) \Rightarrow \omega = \Omega T$$

2.3.8.6A Warping effect:

For low frequencies the relation between Ω and ω is linear i.e., the digital filter have the same amplitude response for high frequencies, however the relation between Ω and ω is non-linear and distortion is introduced. In frequency scale of digital filter this is known as

Warping effect:

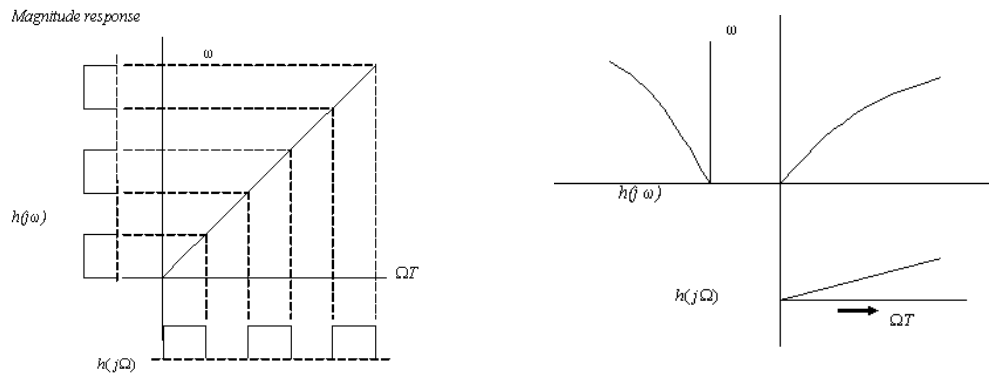


Figure 2.7

Pre-warping:

The warping effect can be eliminated by pre warping the analog filter. This can be done by timing pre warping analog frequencies using formulas.

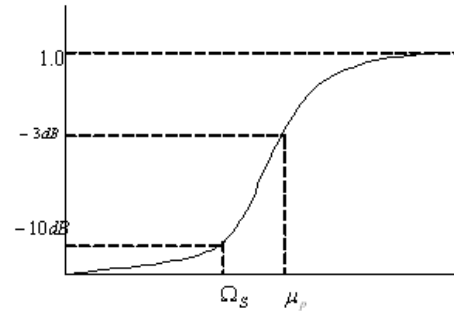
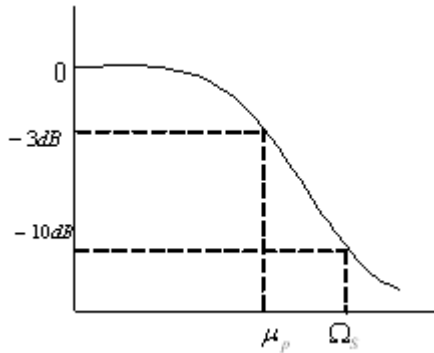
$$\Omega = \frac{2}{T} \tan\left(\frac{\omega}{2}\right)$$

$$\Omega_p = \frac{2}{T} \tan\left(\frac{\omega_p}{2}\right)$$

$$\Omega_s = \frac{2}{T} \tan\left(\frac{\omega_s}{2}\right)$$

Problem 8: Using the bilinear HPF monotonic in pass band cut-off frequency 1000Hz and down 10dB at 350Hz the sampling frequency is 5000Hz.

Sol: $\omega_s = 350 \times 2\pi = 700\pi$



$$\Omega_p = \frac{2}{T} \tan\left(\frac{\omega_p T}{2}\right) = 7265 \text{ rad / s}$$

$$\Omega_s = \frac{2}{T} \tan\left(\frac{\omega_s T}{2}\right) = 7265 \text{ rad / s}$$

, we design LPF, Butter worth

$$N = \frac{\log \sqrt{\frac{10^{0.12\alpha_s}}{10^{0.12\alpha_p}}}}{\log \frac{\Omega_s}{\Omega_p}} = 0.932 \approx 1$$

So, $H(s) = \frac{1}{(s+1)}$; $\Omega_c = \Omega_p = 7265$

$$S \leftarrow \frac{\Omega_s}{S} \Leftrightarrow S \leftarrow \frac{7265}{S}$$

$$= \frac{S}{S + 7265}$$

Using bilinear

$$H(z) = \frac{H(s)}{s} = \frac{2}{T} \left(\frac{z-1}{z+1} \right)$$

$$= \frac{0.5792(1-z^{-1})}{1-0.1584z^{-1}}$$

2.3.8.7 The matched Z-transform:

Another method for converting an analog filter into an equivalent digital filter is to map the poles and zeros of $h(s)$ directly into the poles and zeros in the Z-plane. If

$$H(s) = \frac{\prod_{K=1}^M (s - Z_K)}{\prod_{K=1}^N (s - P_K)}$$

Where $\{Z_K\}$ are the zeros and $\{P_K\}$ are the poles of the filter, then the system function of the digital filter is

$$H(Z) = \frac{\prod_{K=1}^M (1 - e^{Z_K T} Z^{-1})}{\prod_{K=1}^N (1 - e^{P_K T} Z^{-1})}$$

Where T is the sampling interval. Thus each factor of the form $(s-a)$ in $H(s)$ is mapped into the factor $1-e^{aT}Z^{-1}$. This mapping is called the matched Z-transform.

2.3.9 FIR (FINITE IMPULSE RESPONSE) DIGITAL FILTERS:

- Impulse response of these digital filters are computed for finite number of samples and hence called Finite Impulse Response filters.

$$H(n) \neq 0, \quad 0 \leq n \leq M-1$$

= 0, elsewhere

- These filters are characterized by the system function which is not rational

$$H(Z) = \sum_{K=0}^{M-1} B_K Z^{-K}$$
- The present output of these filters does not depend on the previous outputs.
- Have linear phase characteristics and are used in speech processing to eliminate the adverse effects of frequency dispersion due to non-linearity of phase.
- These filters are stable and have greater flexibility to control the shape of their magnitude response and realization efficiency.
- Time delay increase with increase in order of filter.
- The main drawback of an FIR filter is the requirement of higher order for sharp amplitude response.
- FIR filters are unique to the discrete time domain and these cannot be derived from analog filters.

2.3.9.1 Finite Impulse Response Filter Design:

This chapter introduces principles of the finite impulse response (FIR) filter design and investigates the design methods such as the Fourier transform method, window method, frequency sampling method design, and optimal design method. In this chapter, we describe techniques of designing finite impulse response (FIR) filters. An FIR filter is completely specified by the following input-output relationship:

$$y(n) = \sum_{i=0}^K b_i x(n-i)$$

$$= b_0 x(n) + b_1 x(n-1) + b_2 x(n-2) + \dots + b_K x(n-K). \quad [1]$$

where b_i represents FIR filter coefficients and $K + 1$ denotes the FIR filter length. Applying the z-transform on both sides of Equation (1) leads to

$$Y(z) = b_0 X(z) + b_1 z^{-1} X(z) + \dots + b_K z^{-K} X(z) \quad [2]$$

Factoring out $X(z)$ on the right-hand side of Equation (2) and then dividing $X(z)$ on both sides, we have the transfer function, which depicts the FIR filter, as

$$H(z) = \frac{Y(z)}{X(z)} = b_0 + b_1z^{-1} + \dots + b_Kz^{-K} \quad [3]$$

The following example serves to illustrate the notations used in Equations (1) and (3) numerically.

Problem 1: Given the following FIR filter:

$$y(n) = 0.1x(n) + 0.25x(n-1) + 0.2x(n-2)$$

- a. Determine the transform function, filter length, nonzero coefficients, and impulse response.

Ans:

- a. Applying z-transform on both sides of the difference equation yields

$$Y(z) = 0.1X(z) + 0.25X(z)z^{-1} + 0.2X(z)z^{-2}$$

Then the transfer function is found to be

$$H(z) = \frac{Y(z)}{X(z)} = 0.1 + 0.25z^{-1} + 0.2z^{-2}$$

The filter length is $K+1=3$, and the identified coefficients are

$$b_0 = 0.1 \quad b_1 = 0.25 \quad \text{and} \quad b_2 = 0.2$$

Taking the inverse z-transform of the transfer function, we have

$$h(n) = 0.1\delta(n) + 0.25\delta(n-1) + 0.2\delta(n-2).$$

This FIR filter impulse response has only three terms.

The foregoing example is to help us understand the FIR filter format. We can conclude that the transfer function in Equation (3) has a constant term, all the other terms each have a negative power of z , and all the poles are at the origin on the z -plane. Hence, the stability of filter is guaranteed. Its impulse response has only a finite number of terms.

The FIR filter operations involve only multiplying the filter inputs by their corresponding coefficients and accumulating them; the implementation of this filter type in real time is straightforward. From the FIR filter format, the design objective can be to obtain the FIR filter coefficients such that the magnitude frequency response of the FIR filter $H(z)$ will approximate the desired magnitude frequency response, such as that of a lowpass, highpass, bandpass, or bandstop filter. The following sections will introduce design methods to calculate the FIR filter coefficients.

2.3.9 Fourier Transform Design:

We begin with an ideal lowpass filter with a normalized cutoff frequency Ω_c , whose magnitude frequency response in terms of the normalized digital frequency Ω is plotted and is characterized by

$$H(e^{j\Omega}) = \begin{cases} 1, & 0 \leq |\Omega| \leq \Omega_c \\ 0, & \Omega_c \leq |\Omega| \leq \pi \end{cases} \quad [4]$$

Since the frequency response is periodic with a period of $\Omega = 2\pi$ radians, we can extend the frequency response of the ideal filter $H(e^{j\Omega})$, as shown in Figure 12.2. The periodic frequency response can be approximated using a complex Fourier series expansion (see this topic in Appendix B) in terms of the normalized digital frequency Ω , that is, and the Fourier coefficients are given by

$$H(e^{j\Omega}) = \sum_{n=-\infty}^{\infty} c_n e^{-j\omega_0 n \Omega}, \quad [5]$$

And the Fourier coefficients are given by

$$c_n = \frac{1}{2\pi} \int_{-\pi}^{\pi} H(e^{j\Omega}) e^{j\omega_0 n \Omega} d\Omega \quad \text{for } -\infty < n < \infty \quad [6]$$

Notice that we obtain Equations (5) and (6) simply by treating the Fourier series expansion in time domain with the time variable t replaced by the normalized digital frequency variable Ω as shown in Figure 2.8 and Figure 2.9. The fundamental frequency is easily found to be

$$\omega_0 = 2\pi / (\text{period of waveform}) = 2\pi / 2\pi = 1$$

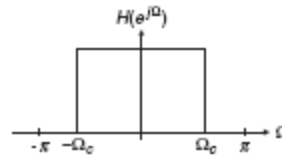


Figure 2.8: Frequency response of an ideal lowpass filter

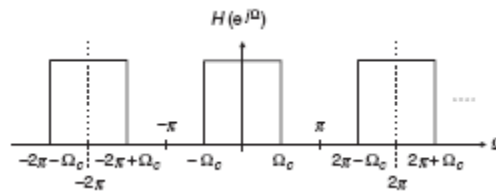


Figure 2.9: Periodicity of the ideal lowpass frequency response.

Substituting $\omega_0 = 1$ into Equation (6) and introducing $h(n) = c_n$, called the desired impulse response of the ideal filter, we obtain the Fourier transform design as

$$h(n) = \frac{1}{2\pi} \int_{-\pi}^{\pi} H(e^{j\Omega}) e^{jn\Omega} d\Omega \quad \text{for } -\infty < n < \infty$$

Now, let us look at the possible z-transfer function. If we substitute $e^{j\Omega} = z$ and $\omega_0 = 1$ back into Equation (5), we yield a z-transfer function in the following format:

$$H(z) = \sum_{n=-\infty}^{\infty} h(n) z^{-n} \quad [9]$$

$$\dots + h(-2)z^2 + h(-1)z^1 + h(0) + h(1)z^{-1} + h(2)z^{-2} + \dots$$

This is a non-causal FIR filter. We will deal with this later in this section. Using the Fourier transform design shown in Equation (8), the desired impulse response approximation of the ideal lowpass filter is solved as

$$h(n) = \frac{1}{2\pi} \int_{-\pi}^{\pi} H(e^{j\Omega}) e^{jn\Omega} d\Omega$$

For $n=0$
$$= \frac{1}{2\pi} \int_{-\pi}^{\pi} 1 d\Omega = \frac{\Omega_c}{\pi}$$

$$h(n) = \frac{1}{2\pi} \int_{-\pi}^{\pi} H(e^{j\Omega}) e^{j\Omega n} d\Omega = \frac{1}{2\pi} \int_{-\Omega_c}^{\Omega_c} e^{j\Omega n} d\Omega$$

For $n \neq 0$

$$= \frac{e^{j\pi n \Omega_c}}{2\pi j n} \Big|_{-\Omega_c}^{\Omega_c} = \frac{1}{\pi n} \frac{e^{j\pi n \Omega_c} - e^{-j\pi n \Omega_c}}{2j} = \frac{\text{Sin}(\Omega_c n)}{\pi n}$$

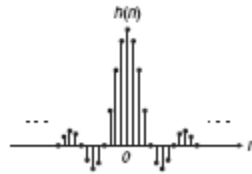


Figure 2.10: Impulse response of an ideal digital low pass filter.

The desired impulse response $h(n)$ is plotted versus the sample number n in Figure 3.

Theoretically, $h(n)$ in Equation (10) exists for $-\infty < n < \infty$ and is symmetrical about $n = 0$; that is, $h(n) = h(-n)$. The amplitude of the impulse response sequence $h(n)$ becomes smaller when n increases in both directions as shown in Figure 2.10. The FIR filter design must first be completed by truncating the infinite-length sequence $h(n)$ to achieve the $2M + 1$ dominant coefficients using the coefficient symmetry, that is,

$$H(z) = b_0 + b_1 z^{-1} + \dots + b_{2M} (2M) z^{-2M} \tag{11}$$

Where the delay operation is given by

$$b_n = h(n - M) \quad \text{for } n = 0, 1, \dots, 2M \tag{12}$$

<p>Filter Type</p>	<p>DEPT. OF ECE Ideal Impulse Response ANNA $H(n0)$ (non-causal FIR coefficients)</p>
--------------------	--

<p>S Low Pass filter</p>	$h(n) = \begin{cases} \frac{\Omega_c}{\pi} & n = 0 \\ \frac{\text{Sin}(\Omega_c n)}{\pi n} & \text{for } n \neq 0 \quad -M \leq n \leq M \end{cases}$
<p>High pass filter</p>	$h(n) = \begin{cases} \frac{\pi - \Omega_c}{\pi} & n = 0 \\ \frac{\text{Sin}(\Omega_c n)}{\pi n} & \text{for } n \neq 0 \quad -M \leq n \leq M \end{cases}$
<p>Band pass filter</p>	$h(n) = \begin{cases} \frac{\Omega_H - \Omega_L}{\pi} & n = 0 \\ \frac{\text{Sin}(\Omega_H n)}{\pi n} - \frac{\text{Sin}(\Omega_L n)}{\pi n} & \text{for } n \neq 0 \quad -M \leq n \leq M \end{cases}$
<p>Band stop filter</p>	$h(n) = \begin{cases} \frac{\pi - \Omega_H + \Omega_L}{\pi} & n = 0 \\ -\frac{\text{Sin}(\Omega_H n)}{\pi n} + \frac{\text{Sin}(\Omega_L n)}{\pi n} & \text{for } n \neq 0 \quad -M \leq n \leq M \end{cases}$

obtain the design equations for other types of FIR filters, such as highpass, bandpass, and band stop, using their ideal frequency responses and Equation (8). The derivations are omitted here. Table 2.1 gives a summary of all the formulas for FIR filter coefficient calculations. The following example illustrates the coefficient calculation for the lowpass FIR filter.

Table 2.1: Summary of ideal impulse responses for standard FIR filter.

2.3.10 Window Method:

In this section, the window method (Fourier transform design with window functions) is developed to remedy the undesirable Gibbs oscillations in the passband and stopband of the designed FIR filter. Recall that Gibbs oscillations

originate from the abrupt truncation of the infinite-length coefficient sequence. Then it is natural to seek a window function, which is symmetrical and can gradually weight the designed FIR coefficients down to zeros at both ends for the range of $-M < n < M$: Applying the window sequence to the filter coefficients gives

$$h_w(n) = h(n).w(n),$$

where $w(n)$ designates the window function.

Common window functions used in the FIR filter design are as follows:

Rectangular window:

$$w_{rec}(n) = 1, \quad -M \leq n \leq M. \quad [15]$$

Triangular (Bartlett) window:

$$w_{tri}(n) = 1 - \frac{|n|}{M}, \quad -M \leq n \leq M. \quad [16]$$

Hanning window:

$$w_{han}(n) = 0.5 + 0.5 \cos\left(\frac{n\pi}{M}\right), \quad -M \leq n \leq M. \quad [17]$$

Hamming window:

$$w_{ham}(n) = 0.54 + 0.46 \cos\left(\frac{n\pi}{M}\right), \quad -M \leq n \leq M. \quad [18]$$

Blackman window:

$$w_{black}(n) = 0.42 + 0.5 \cos\left(\frac{n\pi}{M}\right) + 0.08 \cos\left(\frac{2n\pi}{M}\right), \quad -M \leq n \leq M. \quad [19]$$

In addition, there is another popular window function, called the Kaiser window (its detailed information can be found in Oppenheim, Schafer, and Buck [1999]). As we expected, the rectangular window function has a constant value of 1 within the window, hence does only truncation. As a comparison, shapes of the other window functions from Equations (16) to (19) are plotted in Figure 12.9 for the case of $2M + 1 = 81$ as shown in Figure 2.11.

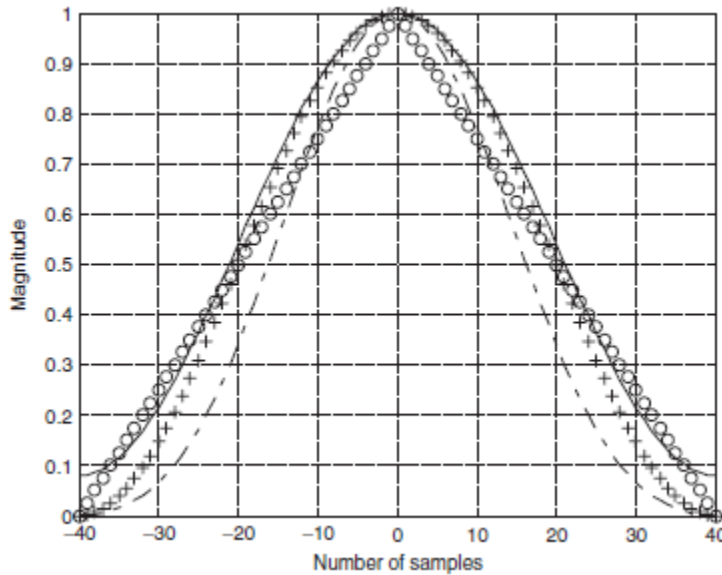


Figure 2.11: Shapes of window functions for the case of $2M+1=81$. O line, Triangular window; +line, Hanning window; Solid line, Hamming window; dashed line, Blackman window.

2.3.10.1 Different Windows:

1. Rectangular window:

The (zero-centered) *rectangular window* may be defined by

$$w_R(n) \triangleq \begin{cases} 1, & -\frac{M-1}{2} \leq n \leq \frac{M-1}{2} \\ 0, & \text{otherwise} \end{cases}$$

where M is the window length in samples (assumed odd for now). A plot of the rectangular window appears in Figure 2.12 for length $M = 21$. It is sometimes convenient to define windows so that their dc gain is 1, in which case we would multiply the definition above by $1/M$.

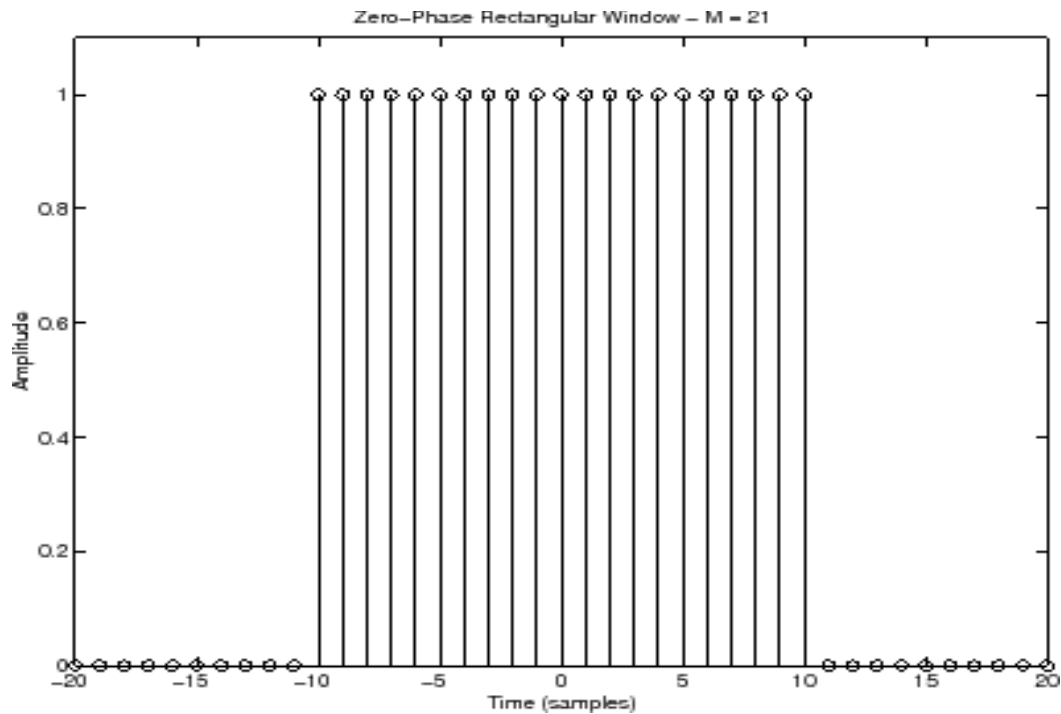


Fig 2.12: Rectangular Window in Time Domain

The rectangular window is rarely used for its low stopband attenuation. The first lobe has attenuation of 13dB and the narrowest transition region as shown in Figure 2.13, therefore. A filter designed using this window has minimum stopband attenuation of 21 dB.

The below Figure illustrates the frequency domain of rectangular window.

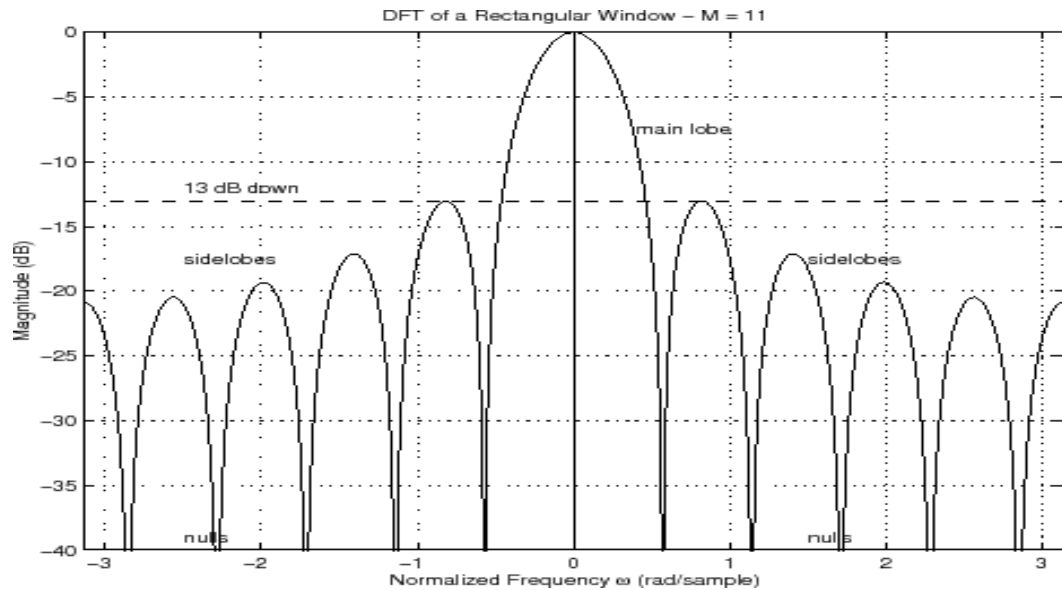


Fig 2.13: Rectangular Window in Frequency Domain

For its less stopband attenuation, the rectangular window is not preferable for digital filter design. Such a less attenuation is a result of cut-off samples within a window (a sequence of sampled frequencies). Up to a zero sample (from which sampling starts), all sampled frequencies are equal to zero. The first sample represents a sudden jump to some value (non-zero sample). Exactly these sudden jumps result in producing relatively sharp high-frequency components which lessen the stopband attenuation.

The attenuation gets higher by making cut-off samples less sharp, which results in reducing filter selectivity, i.e. wider transition region. Since initial requirements of a digital filter are predefined and due to less selectivity, it is necessary to increase the filter order to narrow the transition region. Note the fact that the transition region is inversely proportional to the filter order N . The transition region narrows as the filter order increases.

Increase in filter order affects the filter to become more complex and need more time for sample processing. This is why it is very important to be careful when specifying the window function and filter order as well.

2.Triangular (Bartlett) window:

The triangular (Bartlett) window is one among many functions that lessens the effects of final samples as shown in Figure 2.14. Due to it, the stopband

attenuation of this window is higher than that of the rectangular window, whereas the selectivity is less. Namely, filters designed using this window have wider transition region than those designed using the rectangular window. As a result, it is necessary to have a higher order filter in order to keep the same transition region as that of the filters designed with the rectangular window. This is the price to pay for producing the higher attenuation.

This function also represents a kind of compromise between requirements for as narrow transition region as possible and as higher stopband attenuation as possible, where the transition region is considered more important characteristic.

One of the advantages of designing filter using the triangular window is the simplicity of computing coefficients.

The triangular window coefficients can be expressed as:

$$w[n] = \begin{cases} \frac{2n}{N-1}; & 0 \leq n \leq \frac{N-1}{2} \\ 2 - \frac{2n}{N-1}; & \frac{N+1}{2} \leq n \leq N-1 \end{cases}$$

The below Figure illustrates coefficients in the time-domain.

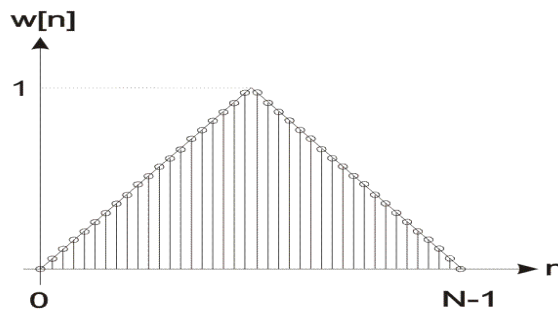


Figure 2.14: Triangular window coefficients in the time-domain

The Figure illustrates the coefficients spectrum of the triangular window shown in above Figure 2.14. Figure 2.15 gives the Triangular (Bartlett) window in the frequency domain (spectrum).

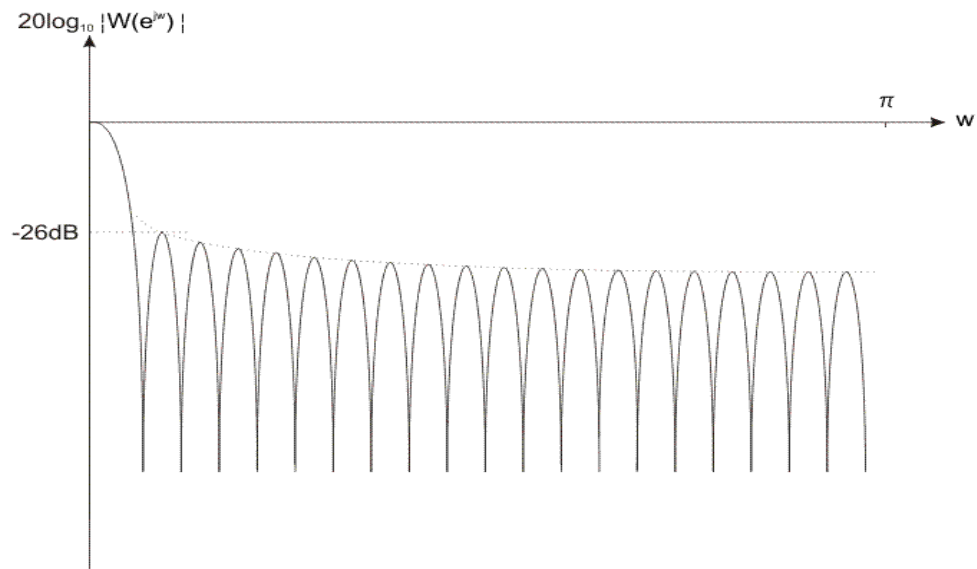


Figure 2.15: Triangular (Bartlett) window in the frequency domain (spectrum)

The attenuation of triangular window is low for most digital filter applications, but it is considerably higher than that for rectangular window. In some cases, when high attenuations are not needed, this filter can be used because it provides an easy way of computing coefficients.

3. Butterworth window:

Regarding window functions used in spectral analysis, the most important performance measures are 3-dB bandwidth and side lobe attenuation. For many window functions, Hanning and Hamming for example, we have no control over a window's 3-dB bandwidth and side lobe attenuation for a given window length. For other window functions—Kaiser, Gaussian, and Chebyshev—we can reduce those windows' 3-dB bandwidth to get improved spectral resolution. However, with these later window functions (what we refer to as “conventional Windows”), spectral resolution improvement comes at the expense of side lobe attenuation reduction that degrades our ability to avoid undesirable spectral leakage. Likewise we can increase those windows' side lobe attenuation, but only by sacrificing desirable spectral resolution. This article describes a novel window function that

enables us to control both its 3-dB bandwidth (spectral resolution) and sidelobe attenuation (spectral leakage) independently.

The 3-dB bandwidth, side lobe attenuation, and roll-off rate are used to measure the performance of windows for power spectral density (PSD) estimation. Improved frequency resolution of the estimated PSD can be obtained if we reduce a window's 3-dB bandwidth. The side lobe attenuation means the difference between magnitude of the main lobe and the maximum magnitude of the sidelobes. The sidelobe roll-off rate is the asymptotic decay rate of sidelobe peaks. Undesirable spectral leakage can be reduced by increasing sidelobe attenuation and roll-off rate. Therefore, an ideal window for PSD estimation has zero bandwidth and infinite sidelobe attenuation such as an impulse function in frequency domain. The conventional windows are able to control 3-dB bandwidth or sidelobe attenuation by only one parameter in general. Thus, they cannot control these two characteristics independently. In other words, if we reduce a window function's 3-dB bandwidth, the sidelobe attenuation is also reduced, and vice versa. This behavior is the cause of the tradeoff problem between good frequency resolution and acceptable spectral leakage in the estimated PSD. The Butterworth window does not have this problem because it allows control of the 3-dB bandwidth and side lobe attenuation independently.

Butterworth windows are used as anti-aliasing filters to reduce the noise in the reconstructed image in previous research. They are also used to remove the edge effect of the matched filter output in pattern matching algorithm. However, in this article, a portion of the impulse response of a Butterworth filter is called the Butterworth window and its characteristics in PSD estimation are analyzed.

The Butterworth window can be obtained by the standard Butterworth filter design procedure. Important to us is the frequency magnitude response $|H(f)|$ of a Butterworth filter, denoted by $H(f)$.

$$|H(f)| = 1 / \sqrt{1 + \left(\frac{f}{f_c}\right)^{2N}},$$

Where f is frequency in hertz. The Butterworth filter is characterized by two independent parameters, 3-dB cutoff frequency f_c and filter order N . The cutoff frequency and order of the Butterworth filter serve as parameters that control the bandwidth and sidelobe attenuation of the Butterworth window. The cutoff frequency of a filter has the identical meaning with the bandwidth of a window. However, the cutoff frequency is represented as a half of the bandwidth since the bandwidth of a window refers to two-sided frequency from negative to positive, while the cutoff frequency of a filter refers to only one-sided positive frequency. Our desired window spectrum is identical to the frequency response of the Butterworth filter. Thus, the inverse Fourier transform is applied to the Butterworth filter's frequency response, in (1), to obtain the filter's impulse response, and a portion of that response becomes the Butterworth window in the time domain.

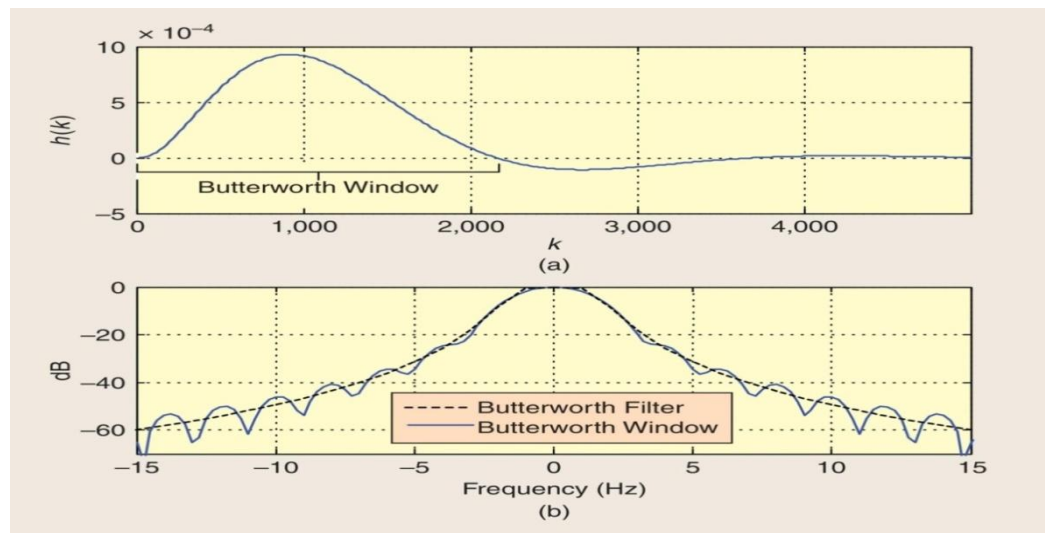


Fig 2.16: Butterworth filter and window: (a) filter impulse response and window function and (b) the filter magnitude response and window spectrum.

In Figure 2.16, Figure (a) shows the time-domain impulse response $h(k)$ of a unity-gain low-pass Butterworth filter when $f_c=0.75$ Hz and $N=3$. In that figure, we show the initial positive-only portion of the impulse response that becomes our desired Butterworth window.

The solid curve in Figure (b) is the frequency spectrum of the 2,139-sample Butterworth window. The 3-dB bandwidth and sidelobe attenuation of this

window are 1.3 Hz and 24.3 dB, respectively. In Figure 1(b), for comparison, we show the frequency magnitude response of the Butterworth filter as the dashed curve.

The frequency characteristics of Butterworth windows with $f_c = 0.75$ Hz are shown in Table 2.2. The sidelobe attenuation is increased from ten to 30.4 dB as the filter order is increased from one to five, while the 3-dB bandwidth is fixed at about 1.5 Hz.

FREQUENCY CHARACTERISTICS OF THE BUTTERWORTH WINDOWS.			
FILTER ORDER	3-DB BANDWIDTH	SIDELobe ATTENUATION	ROLL-OFF RATE
1	1.5 Hz	10.0 dB	
2	1.4 Hz	18.2 dB	
3	1.3 Hz	24.3 dB	-12 dB/OCT.
4	1.3 Hz	28.8 dB	
5	1.3 Hz	30.4 dB	

Table 2.2: Frequency Characteristics of Butterworth Window

3.1 PROPOSED BUTTER WORTH IIR FILTER:

- In this project our main motto is to find a novel IIR filter equation.
- The mathematical formula is given by

$$H(j\Omega) = \frac{1}{\sqrt{\left(1 + \left(\frac{\exp\left(\frac{\Omega}{2.71828}\right)}{\Omega c}\right)^2\right)^{2N}}$$

- The formation for the conventional filter at the cut-off frequency($\Omega=\Omega_c$),The magnitude becomes 0.707 of its equivalent value and steady state error is zero at $\Omega=\text{infinity}(\infty)$.
- Normally we calculating the transfer function with different mathematical function like cosine, sine, tan, log and finally exponential.
- But this transfer function gives the best results compared with other mathematical functions.
- For the standard specifications we get lower order compared with the existed butter worth filter.

Designing LPF Modified Butter worth Filter:

$$N(j\Omega) = \frac{1}{\left[1 + \varepsilon^2 \left(\frac{\exp\left(\frac{\Omega}{\Omega\rho}\right)}{2.71828}\right)^{2N}\right]^{1/2}}$$

$$|N(j\Omega)|^2 = \frac{1}{\left[1 + \varepsilon^2 \left(\frac{\exp\left(\frac{\Omega}{\Omega\rho}\right)}{2.71828}\right)^{2N}\right]}$$

Apply '10 log' both sides

$$20 \log [N(j\Omega)] = 10 \log (1) - 10 \log \left[1 + \varepsilon^2 \left(\frac{\exp\left(\frac{\Omega}{\Omega\rho}\right)}{2.71828} \right)^{2N} \right]$$

At $\Omega = \Omega\rho$ the attenuation equal to ' α_ρ '

So,

$$20 \log [N(j\Omega)] = -\alpha_\rho = -10 \log (1 + \varepsilon^2)$$

$$0.1 \alpha_\rho = \log (1 + \varepsilon^2)$$

$$\varepsilon^2 = 10^{0.1 \alpha_\rho} - 1$$

$$\varepsilon = \left(10^{0.1 \alpha_\rho} - 1 \right)^{1/2}$$

At $\Omega = \Omega_s$, the attenuation is ' α_s '

$$20 \log [N(j\Omega)] = -\alpha_s = -10 \log \left[1 + \varepsilon^2 \left(\frac{\exp\left(\frac{\Omega}{\Omega\rho}\right)}{2.71828} \right)^{2N} \right]$$

$$\left(1 + \varepsilon^2 \left(\frac{\exp\left(\frac{\Omega}{\Omega\rho}\right)}{2.71828} \right)^{2N} \right) = 10^{0.1 \alpha_s}$$

$$\varepsilon^2 \left(\frac{\exp\left(\frac{\Omega}{\Omega\rho}\right)}{2.71828} \right)^{2N} = 10^{0.1 \alpha_s} - 1$$

$$\left(10^{0.1 \alpha_\rho} - 1 \right) \left(\frac{\exp\left(\frac{\Omega}{\Omega\rho}\right)}{2.71828} \right)^{2N} = 10^{0.1 \alpha_s} - 1$$

$$N \log \left(\frac{\exp\left(\frac{\Omega}{\Omega\rho}\right)}{2.71828} \right) = \log \sqrt{\frac{10^{0.1\alpha_s} - 1}{10^{0.1\alpha_p} - 1}}$$

$$N \geq \frac{\log \sqrt{\frac{10^{0.1\alpha_s} - 1}{10^{0.1\alpha_p} - 1}}}{\log \left(\frac{\exp\left(\frac{\Omega}{\Omega\rho}\right)}{2.71828} \right)}$$

$$N \geq \frac{\log \sqrt{\frac{\lambda}{\varepsilon}}}{\log \left(\frac{\exp\left(\frac{\Omega}{\Omega\rho}\right)}{2.71828} \right)}$$

where $\lambda = \sqrt{(10^{0.1\alpha_s} - 1)}$
 $\varepsilon = \sqrt{(10^{0.1\alpha_p} - 1)}$

α_p = pass band attenuation

α_s = stop band attenuation

$\Omega\rho$ = pass band frequency

Ω_s = stop band frequency

3.2 IIR (INFINITE IMPULSE RESPONSE) DIGITAL FILTERS:

In this project, the following equation used as an IIR filter. This is the exponential function.

$$H(j\Omega) = \frac{1}{\sqrt{\left(1 + \left(\frac{\exp\left\{\frac{\Omega}{\Omega_c}\right\}}{2.71828}\right)^2\right)^{2N}}}$$

Where Ω = variable frequency,

Ω_c =cut-off frequency,

N= order.

The formation for the conventional filter at the cut-off frequency($\Omega=\Omega_c$),The magnitude becomes 0.707 of its equivalent value and steady state error is zero at $\Omega=\infty$.

The discrete-time transfer function $H_d(Z)$ of an IIR digital filter is obtained from continuous transfer function $H_a(S)$ of an analog filter. The approximation is obtained using one of the following methods:

- Approximation of derivatives
- Impulse Response Invariance method
- The matched Z-transform
- Bilinear transformation method

In this methods, we used the Bilinear transforming technique for the poles of an IIR filter.

3.2.1 INTEGER ORDER TRANFER FUNCTION: This can be characterized by differential equation

$$H(j\Omega) = \frac{1}{\sqrt{\left(1 + \epsilon^2 \left(\frac{\exp\left\{\frac{\Omega}{\Omega_c}\right\}}{2.71828}\right)^2\right)^{2N}}}$$

$$|H(s)| = \frac{1}{\sqrt{\left(1 + \epsilon^2 \left(\frac{e^s}{2.71828}\right)\right)^{2Ns}}}$$

From the expansion of e^x ,

$$e^x = 1 + \frac{x}{1!} + \frac{x^2}{2!} + \frac{x^3}{3!} + \dots, -\infty < x < \infty$$

$$|H(s)| = \frac{1}{\sqrt{\left(1 + \frac{\epsilon^2}{(2.718)^{2N}} \left[1 + \frac{s}{1!} + \frac{s^2}{2!} + \frac{s^3}{3!} + \dots\right]\right)^4}}$$

$$|H(s)|^2 = \frac{1}{1 + \frac{\epsilon^2}{(2.718)^4} \left[1 + \frac{4s}{1!} + \frac{16s^2}{2} + \frac{64s^3}{6} + \dots\right]} \longrightarrow 1$$

$$|H(s)|^2 = \frac{1}{a_4s^4 + a_3s^3 + a_2s^2 + a_1s^1 + a_0} \longrightarrow 2$$

Write the equation 1 as equation 2,s

$$|H(s)|^2 = \frac{1}{1 + \frac{0.5848}{(54.5981)} [1 + 4s + 8s^2 + 10.67s^3 + \dots]}$$

$$= \frac{1}{0.114s^4 + 0.114s^3 + 0.085s^2 + 0.0428s + 1.011}$$

To find the poles of above equation,

$$0.114s^4 + 0.114s^3 + 0.085s^2 + 0.0428s + 1.011 = 0$$

Poles:

$$-1.4296 + 1.2449j,$$

$$-1.4296 - 1.2449j,$$

$$0.9296+1.2664j,$$

$$0.9296-1.2664j.$$

For a stable system, we need to take the roots on the negative or left side of the s plane,

$$S_1=-1.4296+1.2449i$$

$$S_2=-1.4296-1.2449i$$

The transfer function of an IIR filter is given by,

$$H|s| = \frac{1}{(s+1.4296-1.2449i)(s+1.4296+1.2449i)}$$

$$= \frac{1}{s^2+s(2.8592)+3.5934}$$

$$W_c=w_p\varepsilon^{(-1/N)}$$

$$=20(0.764)^{(-1/2)}$$

$$=22.88\text{rad/sec}$$

Put $s=s/w_c$

$$= \frac{1}{\left(\frac{s}{22.88}\right)^2 + (2.8592)\frac{s}{22.88} + 3.5934}$$

$$= \frac{523.4944}{s^2+s(65.418)+1881.124777}$$

3.2.2 FRACTIONAL ORDER TRANSFER FUNCTION:

For $N = \frac{P}{Q}$ order, we get $\frac{1}{Q}=q$

We know that,

$$H(j\Omega) = \frac{1}{\sqrt{\left(1 + \left(\frac{\exp\left\{j\left(\frac{\Omega}{\Omega_c}\right)\right)}{2.71828}\right)\right)^{2N}}}$$

$$H(-j\Omega)H(j\Omega) = \frac{1}{\sqrt{\left(1 + \left(\frac{\exp\left\{j\left(\frac{\Omega}{\Omega_c}\right)\right)}{2.71828}\right)\right)^{2N}}}$$

$$\Omega = \frac{s}{j}$$

$$H(-s)H(s) = \frac{1}{\sqrt{\left(1 + \left(\frac{\exp\left\{j\left(\frac{s}{\Omega_c}\right)\right)}{2.71828}\right)\right)^{2N}}}$$

Putting $\Omega = s * q$

$$H(-\Omega)H(\Omega) = \frac{1}{\sqrt{\left(1 + \left(\frac{\exp\left\{j\left(\frac{2sN}{\Omega_c}\right)\right)}{2.71828^2}\right)\right)^p}}$$

Now equating this characteristic equation to zero,

$$1 + \left(\frac{\exp\left\{j\left(\frac{2\Omega}{\Omega_c}\right)\right\}}{2.71828^2}\right)^p = 0$$

$$\frac{\exp\left\{j\left(\frac{2\Omega p}{\Omega_c}\right)\right\}}{\exp^{2p}} = (-1)$$

$$\exp\left\{j\left(\frac{\Omega}{\Omega_c} - 1\right)2p\right\} = \exp^{j(2k-1)\pi}$$

Bases are equal powers must be equated,

$$\left(\frac{\Omega}{j\Omega_c}-1\right)2p=j(2k-1)\pi$$

Therefore,

$$\Omega_k=j\Omega_c\left(1+\frac{j(2k-1)\pi}{2p}\right)$$

We know that,

$$P=7$$

$$\begin{aligned}\Omega_1 &= j\Omega_c\left(1+\frac{j\pi}{14}\right) \\ &= \left(\frac{-\pi}{14} + j\right)\Omega_c\end{aligned}$$

$$\begin{aligned}\Omega_2 &= j\Omega_c\left(1+\frac{j3\pi}{14}\right) \\ &= \left(\frac{-3\pi}{14} + j\right)\Omega_c\end{aligned}$$

$$\begin{aligned}\Omega_3 &= j\Omega_c\left(1+\frac{j5\pi}{14}\right) \\ &= \left(\frac{-5\pi}{14} + j\right)\Omega_c\end{aligned}$$

$$\begin{aligned}\Omega_4 &= j\Omega_c\left(1+\frac{j7\pi}{14}\right) \\ &= \left(\frac{-7\pi}{14} + j\right)\Omega_c\end{aligned}$$

$$\begin{aligned}\Omega_5 &= j\Omega_c\left(1+\frac{j9\pi}{14}\right) \\ &= \left(\frac{-9\pi}{14} + j\right)\Omega_c\end{aligned}$$

$$\Omega_6=j\Omega_c\left(1+\frac{j11\pi}{14}\right)$$

$$= \left(\frac{-11\pi}{14} + j\right)\Omega_c$$

$$\Omega_7 = j\Omega_c \left(1 + \frac{j13\pi}{14}\right)$$

$$= \left(\frac{-13\pi}{14} + j\right)\Omega_c$$

$$H(s) =$$

$$\frac{1}{\left(0.1s - \left(\frac{-\pi}{14} + j\right)\Omega_c\right)\left(0.1s - \left(\frac{-3\pi}{14} + j\right)\Omega_c\right)\left(0.1s - \left(\frac{-5\pi}{14} + j\right)\Omega_c\right)\left(0.1s - \left(\frac{-7\pi}{14} + j\right)\Omega_c\right)\left(0.1s - \left(\frac{-9\pi}{14} + j\right)\Omega_c\right)\left(0.1s - \left(\frac{-11\pi}{14} + j\right)\Omega_c\right)\left(0.1s - \left(\frac{-13\pi}{14} + j\right)\Omega_c\right)}$$

The figures shows the IIR filter responses.

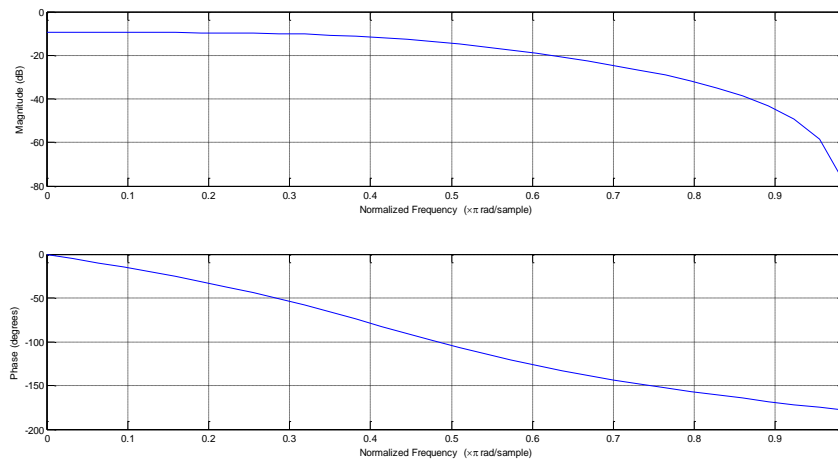


Figure 3.1: waveform of IIR filter

The following Figure 3.1 shows the z-plane of the IIR filter. The all poles are placed inside of the unit plane. So the system is stable.

3.3 Comparison of Butter worth & Novel Butterworth filter:

Table 3.1: Comparison of Butterworth & Novel Butterworth filter

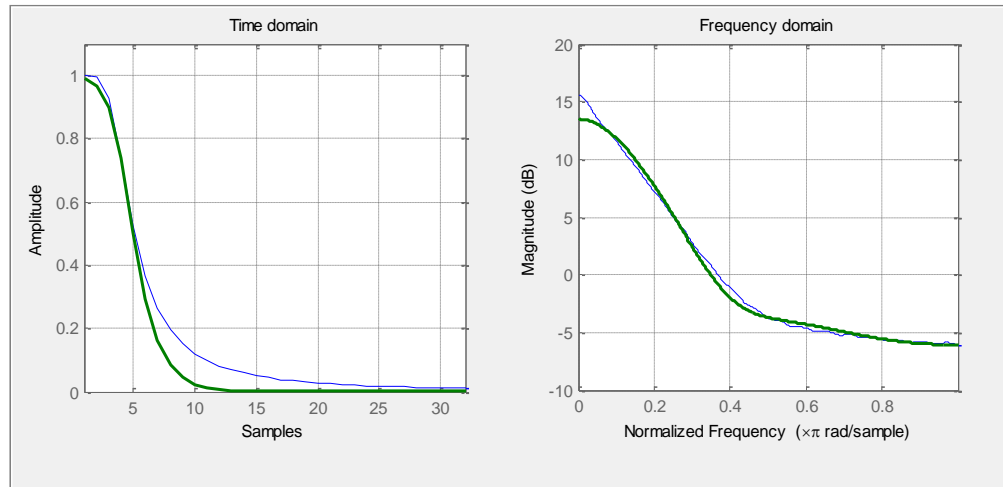
--	--

Butter worth filter	Novel Butter worth filter
<ul style="list-style-type: none"> • The Butter worth filter equation is given by, $H(j\Omega) = \frac{1}{\sqrt{\left(1 + \left(\frac{\Omega}{\Omega_c}\right)^{2N}\right)}}$ <p style="text-align: center;">Where Ω = variable frequency, Ω_c=cut-off frequency, N= order.</p> • For specific order. • Flat response in pass band • Cut-off frequencies are easily find out due to flat response. • No ripples in transition band 	<ul style="list-style-type: none"> • The Novel Butter worth filter equation is given by, $H(j\Omega) = \frac{1}{\sqrt{\left(1 + \left(\frac{\exp\left(\frac{\Omega}{2.71828}\right)}{\Omega_c}\right)^{2N}\right)}}$ <p style="text-align: center;">Where Ω = variable frequency, Ω_c=cut-off frequency, N= order.</p> • Order decreases. • More flat response compared to butter worth • Cut-off frequencies are accurately find out due to more flat response. • No ripples in transition band

The Table 3.1 gives the major comparisons of the two Butterworth Filters.

Waveforms of butter worth and novel butter worth filters:

The Figure 3.2 shows the output waveforms of the two filters.



Novel ■ butter worth filter Butterworth ■ lter

Figure 3.2: waveforms of filters

3.4 Novel window:

- Here the novel butter worth filter transfer function is used as a novel butter worth window function.
- The formula is given by,

$$mbw(w) = H(j\Omega) = \frac{1}{\sqrt{\left(1 + \left(\frac{\exp\left(\frac{k1}{k2}\right)}{2.71828}\right)^2\right)^{2N}}}$$

Where k1 is variable frequency,

k2 is cut-off frequency and

N is the order of the filter.

- In this window analysis the spectral parameters are controlled by cut-off frequency and order
- But where as in conventional windows no controlled parameters to analyze the spectral paramet

- The following Table 3.2 is the frequency characteristics of novel butterworth filter on comparison with the original Butterworth Filter.

Table 3.2: frequency characteristics of novel butter worth filter

CUT OFF FREQUENCIES	BUTTERWORTH WINDOW(SIDELOBE ATTENUATION)	NOVEL WINDOW FUNCTION(SIDE LOBE ATTENUATION)
0.3 π	-19.8dB	-27.5dB
0.4 π	-18.3dB	-18.1dB
0.5 π	-18.9dB	-18.7dB
0.4 π	-19.2dB	-18.5dB
0.5 π	-18.5dB	-18.1dB
0.6 π	-19dB	-18.4dB
0.5 π	-17.8dB	-17.4dB
0.6 π	-18.3dB	-17.7dB

- The spectral characteristics of novel butterworth filter at different cut-off frequencies and different orders.
- At $N=2$ $\omega_c=0.3*\pi$

FEATURE EXTRACTION OF EARTHQUAKE SIGNALS USING FRACTIONAL DOMAIN

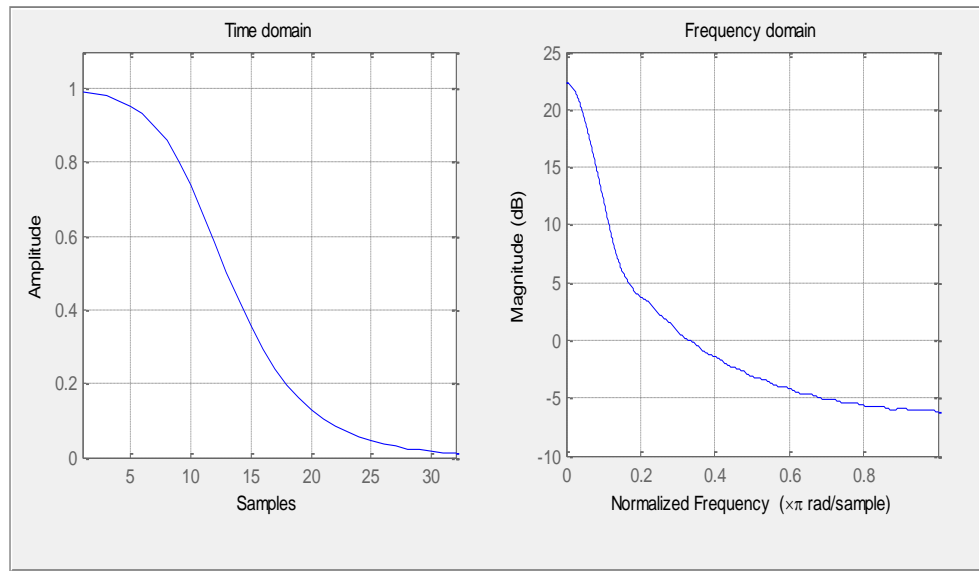


Fig (a)

➤ At $N=2$ $\omega_c=0.4*\pi$

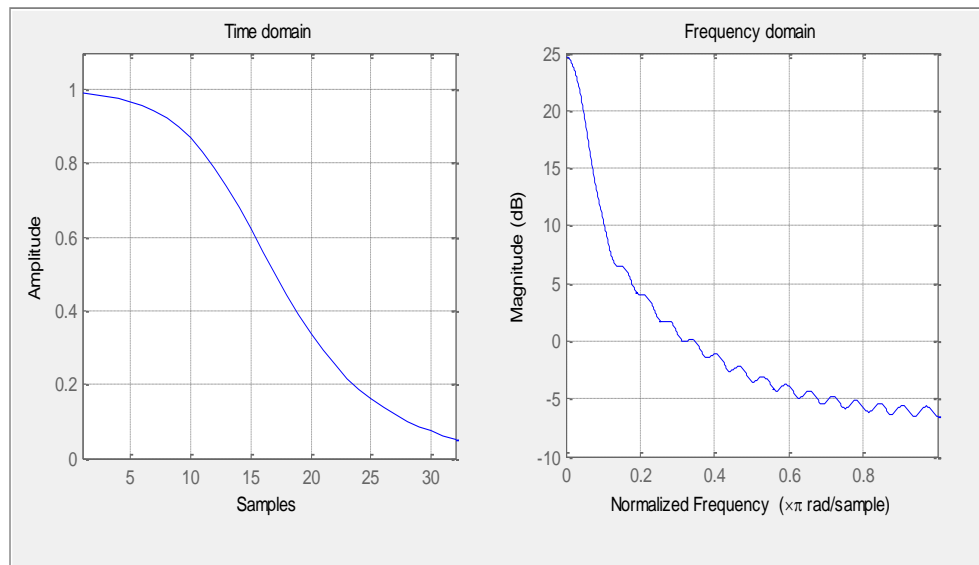


Fig (b)

• At $N=3$ $\omega_c=0.4*\pi$

FEATURE EXTRACTION OF EARTHQUAKE SIGNALS USING FRACTIONAL DOMAIN

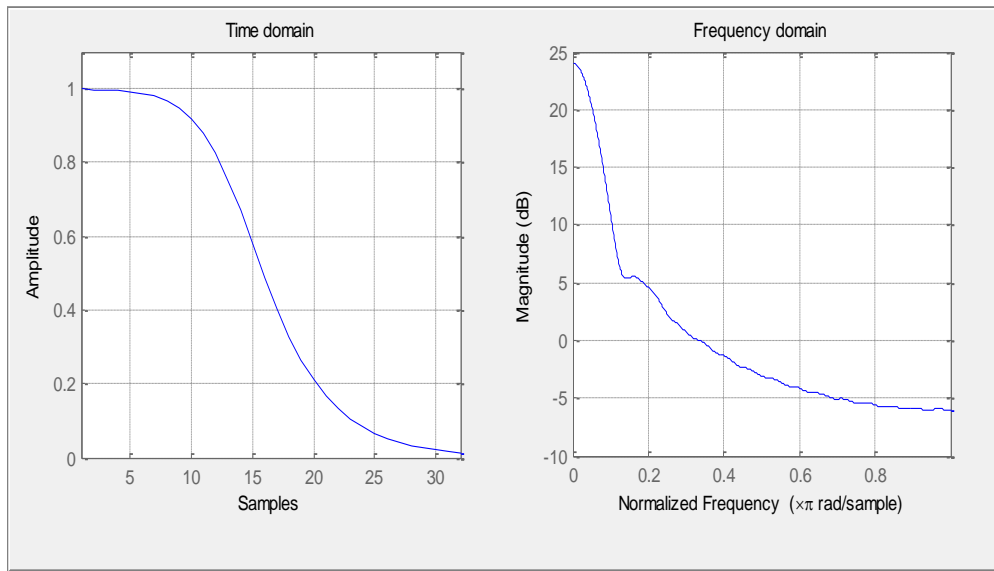


Fig (c)

- At $N=3$ $\omega_c = 0.5\pi$

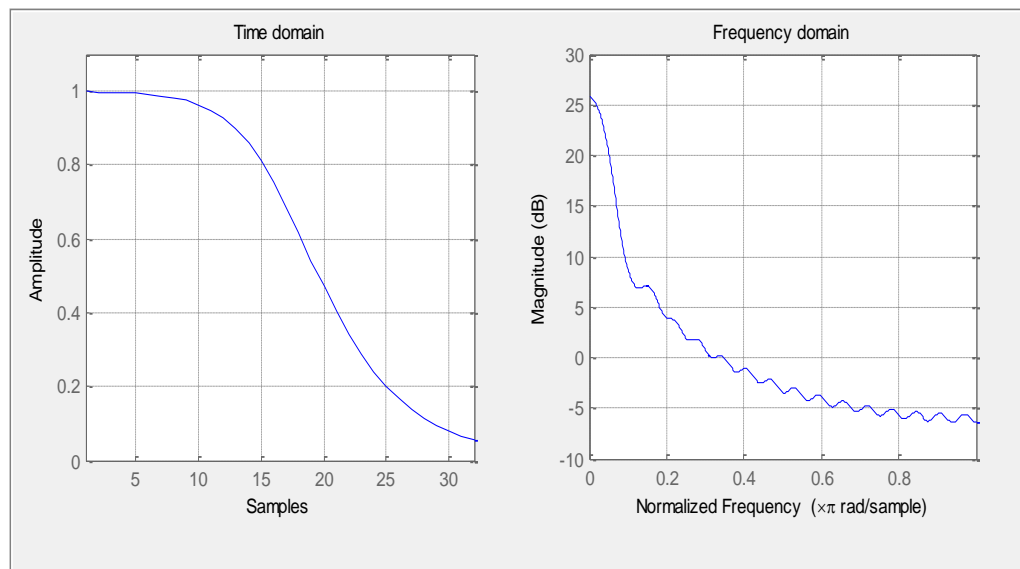


Fig (d)

- At $N=4$ $\omega_c = 0.5\pi$

FEATURE EXTRACTION OF EARTHQUAKE SIGNALS USING FRACTIONAL DOMAIN

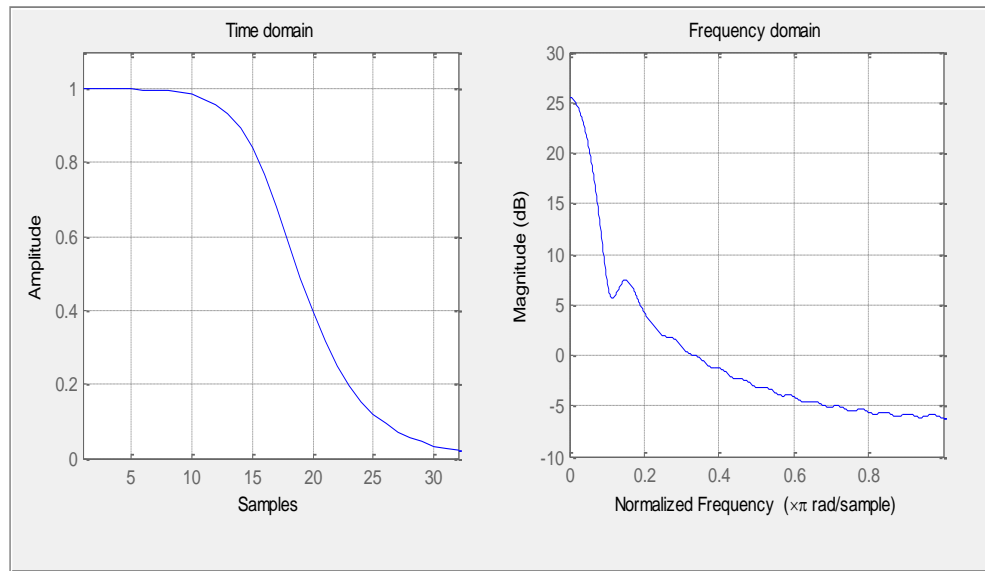


Fig (e)

- At $N=4$ $w_c=0.6*\pi$

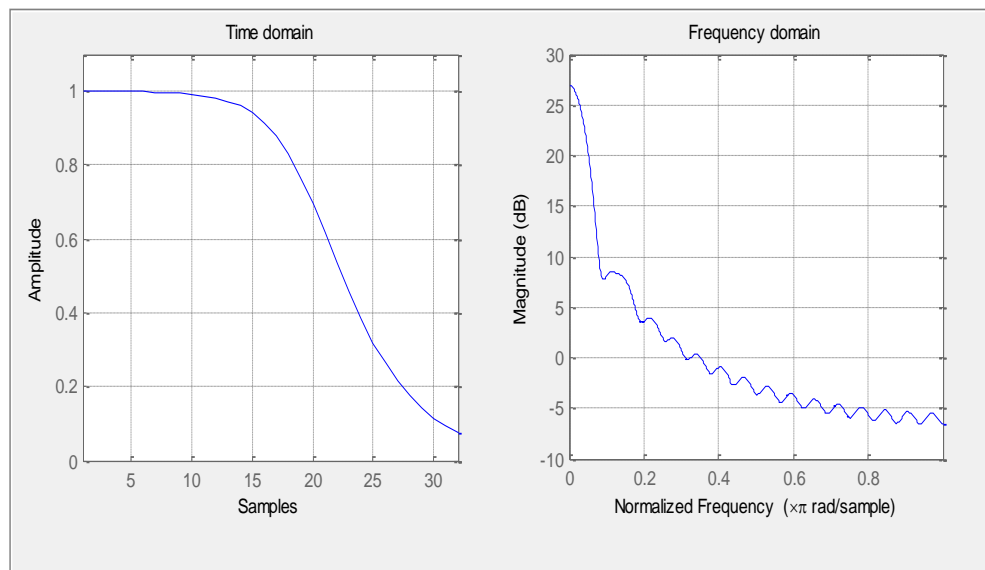


Fig (f)

- At $N=5$ $w_c=0.5*\pi$

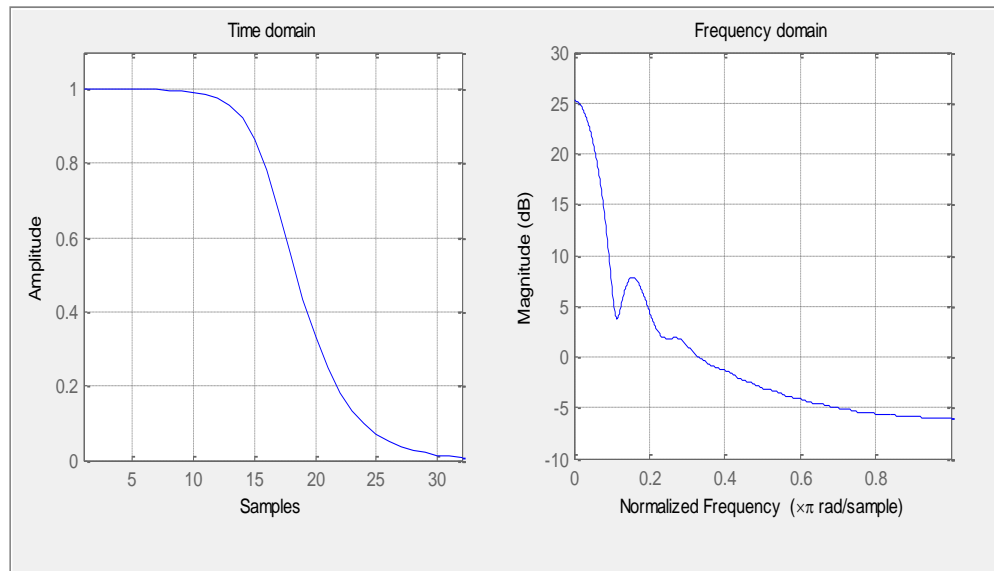


Fig (g)

- At $N=5$ $w_c=0.6*\pi$

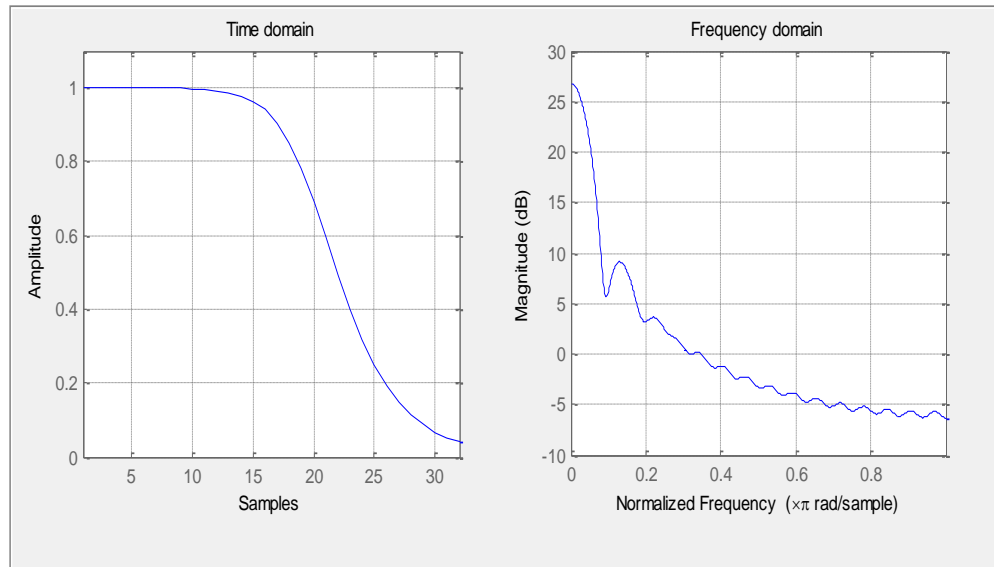


Fig (h)

Figure 3.3(a,b,c,d,e,f,g,h):waveforms of novel window

3.5 Comparison of frequency characteristics of different windows:

T

WINDOW	3-dBBANDWIDTH	SIDE LOBE ATTENUATION
Rectangular	0.879 Hz	-13.3dB
Triangular	1.270 Hz	-26.5 dB
Butterworth (fc =0.439 Hz)		
N=2	0.793 Hz	-18.2 dB
N=3	0.740 Hz	-24.3dB
N=4	0.731 Hz	-28.8 dB
Novel Butterworth (fc= 0.439Hz)		
N =2	0.09375	-27.5dB
N=3	0.11719	-18.6dB
N=4	0.125	-18dB

on of frequency characteristics

The above Table 3.3 shows the frequency characteristics of conventional windows, Butterworth window and novel Butterworthwindow. The conventional windows are able to control 3-dB bandwidth or side lobe attenuation by only one parameter in general. Thus, they cannot control these two characteristics independently. In other words, if we reduce a window function’s 3-dB bandwidth, the side lobe attenuation is also reduced, and vice versa. Butterworth window function that enables us to control both its 3-dB bandwidth (spectral resolution) and sidelobe attenuation (spectral leakage) independently. In this window analysis the spectral parameters are controlled by cut-off frequency and order

3.6 FIR FILTER:

- Impulse response of these digital filters are computed for finite number of samples and hence called Finite Impulse Response filters.

$$H(n) \neq 0, \quad 0 \leq n \leq M-1$$

$$= 0, \quad \text{elsewhere}$$

- In this we designed the FIR filter by using window function.
- After multiplying novel window sequence $w(n)$ with $hd(n)$, we get a finite duration sequence $h(n)$ that satisfies the desired magnitude response.

$$h(n) = hd(n)w(n) \quad \text{for all } |n| \leq \{N-1/2\}$$

$$= 0 \quad \text{for } |n| > \{N-1/2\}$$

Where $hd(n)$ is the IIR filter,

$w(n)$ is the novel Window function.

- Waveforms of the FIR filter at different cut-off frequencies as shown in fig 3.4
- At $\omega_c=0.5\pi$, $N=2$

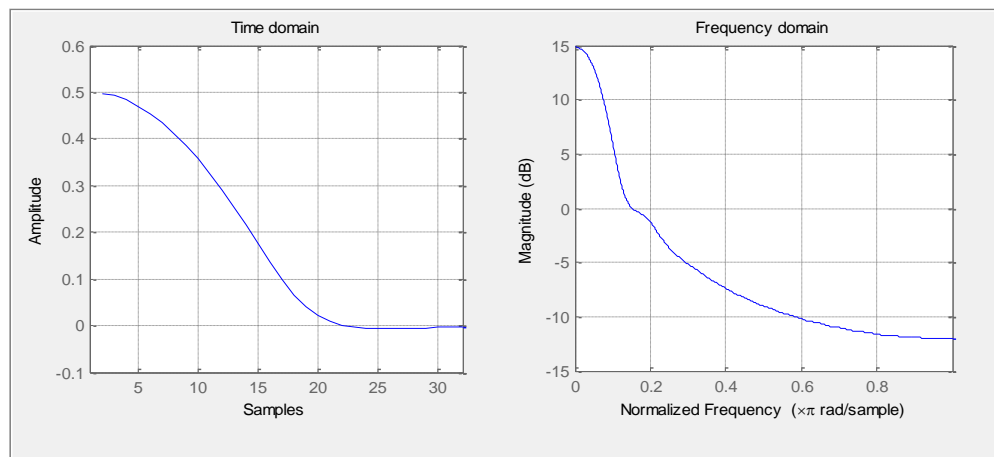


Fig (a)

- At $\omega_c=0.9\pi$, $N=2$

FEATURE EXTRACTION OF EARTHQUAKE SIGNALS USING FRACTIONAL DOMAIN

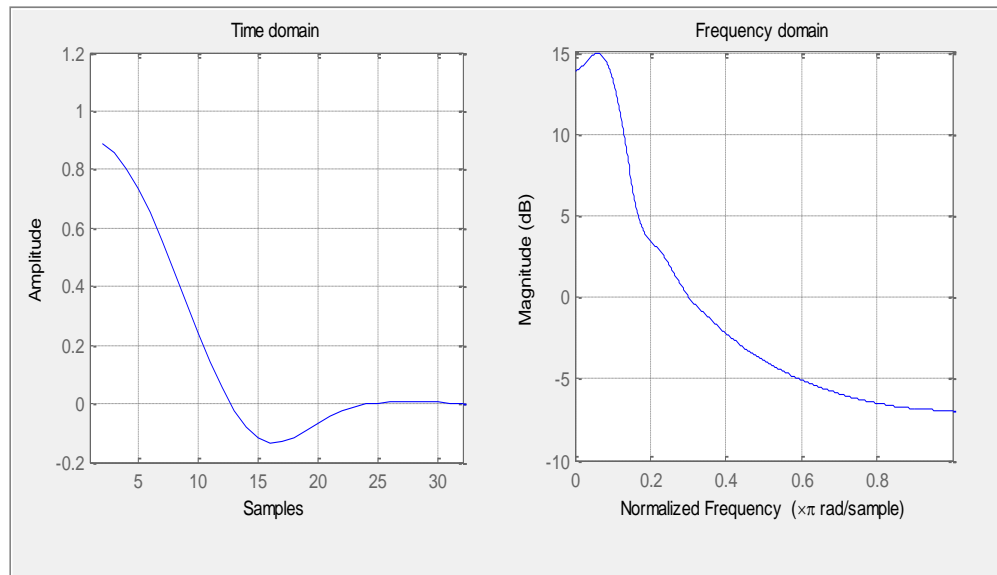


Fig (b)

- At $\omega_c=0.5$, $N=4$

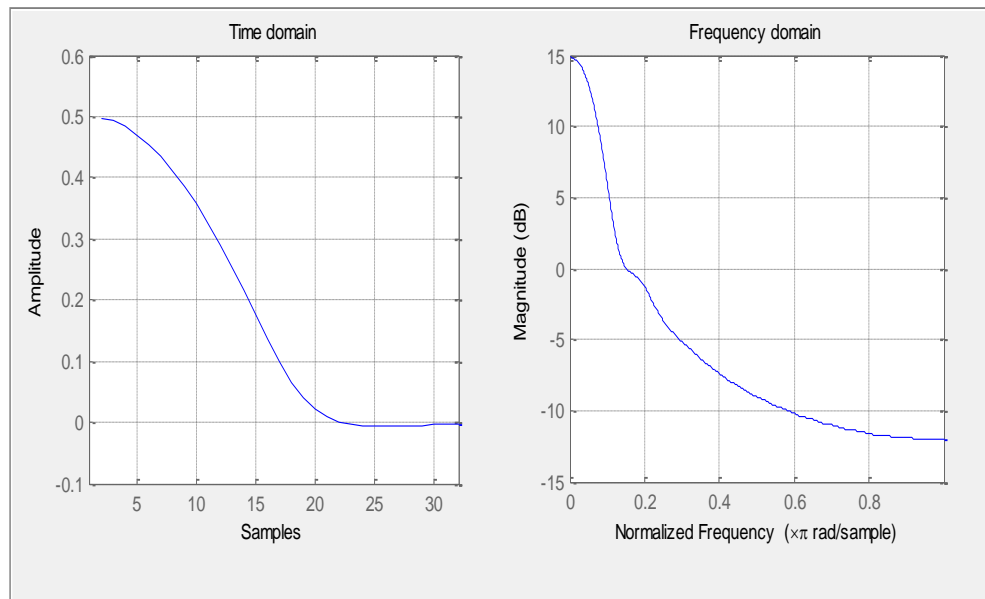


Fig (c)

- At $\omega_c=0.9$, $N=4$

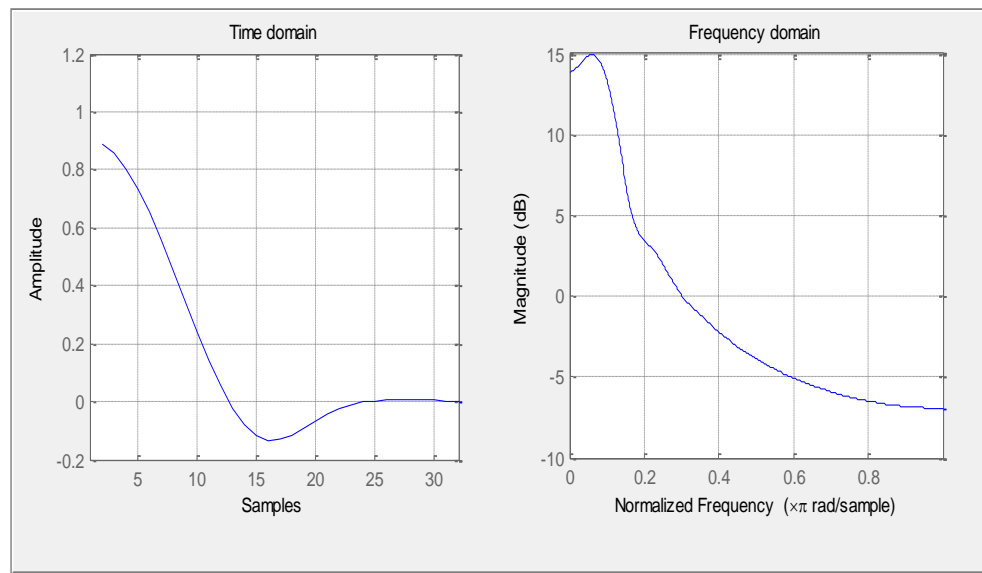


Fig (d)

Fig 3.4(a, b, c, d): wave forms of FIR filter

4.1 SIGNAL TO NOISE RATIO CALCULATION:

Signal to noise ratio is a measure (SNR) used in science and engineering that compares the level of a desired signal to the level of background noise. It is defined as the ratio of signal power with the noise power. It is often expressed in dB. The SNR ratio, when greater than 1:1 indicates more signal than noise in the detected output signal.

$$SNR = \frac{P_{signal}}{P_{noise}}$$

Where P is average power, Both signal and noise power must be measured at the same and equivalent points in a system, and within the same system bandwidth.

If the variance of the signal and noise are known, and the signal is zero-mean.

$$SNR = \frac{\sigma_{signal}^2}{\sigma_{noise}^2}$$

If the signal and the noise are measured across the same impedance then the SNR can be obtained by calculating the square of the amplitude ratio,

$$SNR = \frac{P_{signal}}{P_{noise}} = \left(\frac{A_{signal}}{A_{noise}} \right)^2$$

Where A is root mean square (RMS) amplitude

While SNR is commonly quoted for electrical signals, it can be applied to any form of signal (such as isotope levels in an ice core or biochemical signaling between cells). The signal-to-noise ratio, the bandwidth, and the channel capacity of a communication channel are connected by the Shannon–Hartley theorem.

Signal-to-noise ratio is sometimes used informally to refer to the ratio of useful information to false or irrelevant data in a conversation or exchange.

Because many signals have a very wide dynamic range, signals are often expressed using the logarithmic decibel scale. Based upon the definition of decibel, signal and noise may be expressed in decibels (dB) as

$$P_{signal, dB} = 10 \log_{10}(P_{signal})$$

And

$$P_{noise, dB} = 10 \log_{10}(P_{noise})$$

In a similar manner, SNR may be expressed in decibels as

$$SNR_{dB} = 10 \log_{10}(SNR)$$

Using the definition of SNR

$$SNR_{dB} = 10 \log_{10} \left(\frac{P_{signal}}{P_{noise}} \right)$$

Using the quotient rule for logarithms

$$10 \log_{10} \left(\frac{P_{signal}}{P_{noise}} \right) = 10 \log_{10}(P_{signal}) - 10 \log_{10}(P_{noise})$$

Substituting the definitions of SNR, signal, and noise in decibels into the above equation results in an important formula for calculating the signal to noise ratio in decibels, when the signal and noise are also in decibels:

$$SNR_{dB} = P_{signal, dB} - P_{noise, dB}$$

In the above formula, P is measured in units of power, such as Watts or milliwatts and signal-to-noise ratio is a pure number. However, when the signal and noise are

measured in Volts or Amperes, which are measures of amplitudes, they must be squared to be proportionate to power as shown below.

$$SNR_{dB} = 10 \log_{10} \left[\left(\frac{A_{signal}}{A_{noise}} \right)^2 \right] = 20 \log_{10} \left(\frac{A_{signal}}{A_{noise}} \right) = (A_{signal,dB} - A_{noise,dB}) .$$

Results & Implementations:

Conventional Butterworth Filter:

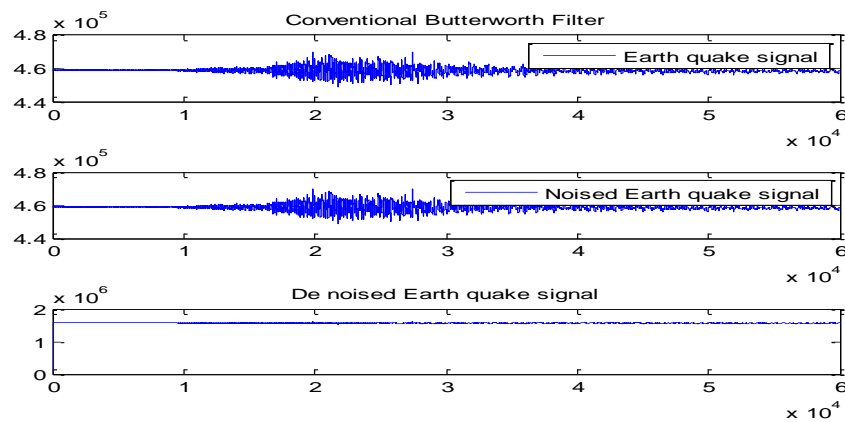


Fig:

Integer order Modified Butterworth Filter:

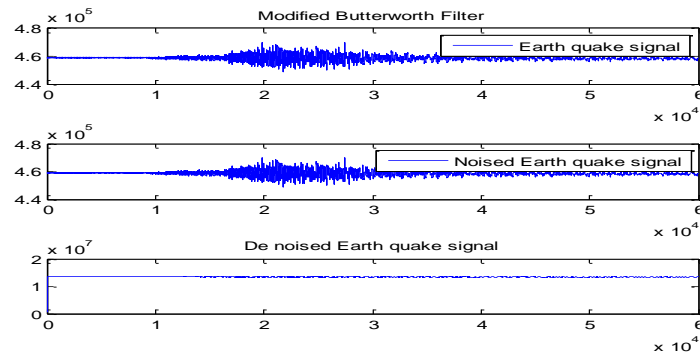


Fig:

Fractional order Butterworth Filter

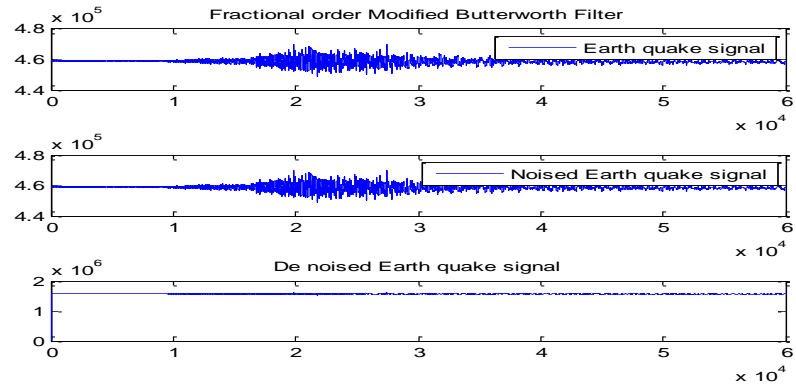


Fig:

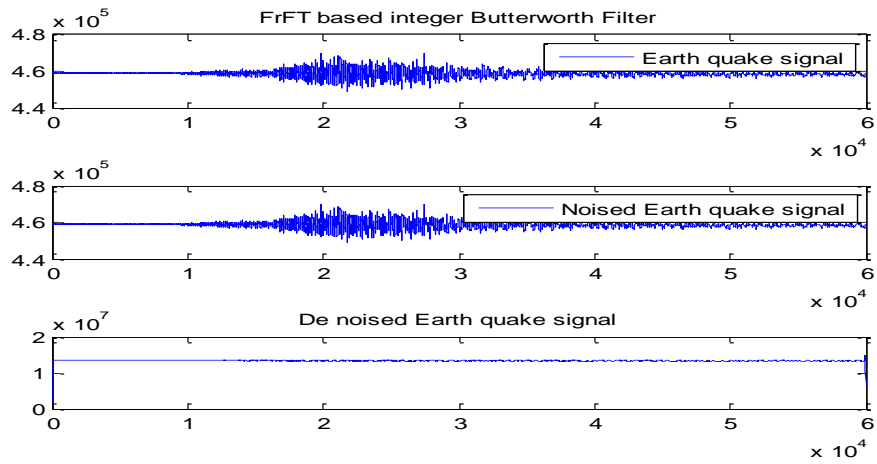


Fig:

FEATURE EXTRACTION OF EARTHQUAKE SIGNALS USING FRACTIONAL DOMAIN

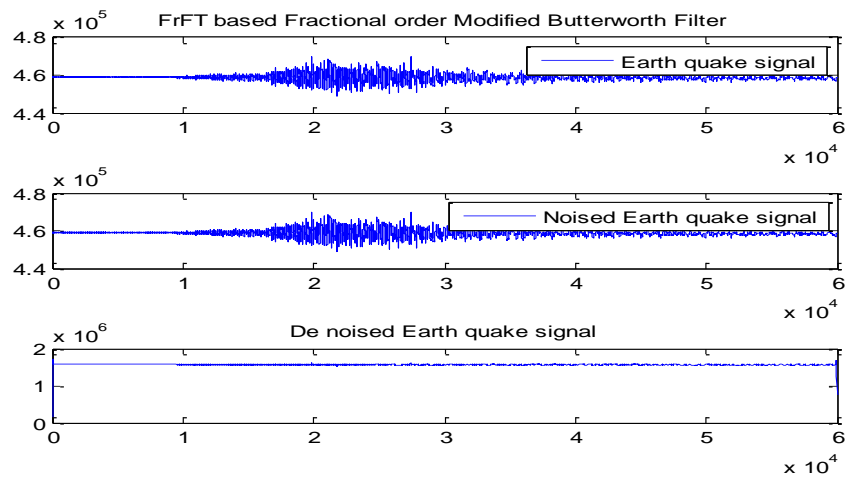


Fig:

Performance of SNR

S.NO	TYPE OF BUTTERWORTH FILTER	OUPUT SNR IN dB
1	Conventional	1.0013
2	Integer order	1.0725
3	Fractional order	1.9988

4.2 SNR CALCULATION USING MATLAB:

Conventional Butterworth Filter:

```
clc;  
clearall;  
closeall;  
load'earth.txt'  
time= 1:1:60000;  
x1=earth(:,3)';  
noise=(sin(2.*pi.*5500.*time./100));
```

```
x2=x1+noise;
b=[0.0334 0 -0.1334 0 0.2000 0 -0.1334 0 0.334];
a=[1.0000 -4.6508 9.5554 -11.6600 9.4856 -5.2835 1.9256 -0.4155 0.0434];
y1=filter (b, a, x1);
opsnr=((abs(y1.*y1))/(abs((y1-x2).*(y1-x2))))
subplot (3,1,1);
plot(x1);
subplot (3,1,2);
plot(x2);
subplot (3,1,3);
plot (y1);
Output:
opsnr = 1.0013
```

Modified Novel Butterworth Filter:

Integer Order:

```
clc;
clearall;
closeall;
load'earth.txt'
x1=earth(:,3)';
time=1:1:60000;
noise=(sin(2.*pi.*5500.*time./100));
x2=x1+noise;
k1=0:0.1:pi;
k2=1*pi;N=2;
h=1./(1+(((exp((k1/k2))/2.71828).^2*N))).^5;
h1=filter(h,1,x1);
opsnr=((abs(h1.*h1))/(abs((h1-x2).*(h1-x2))))
subplot (3,1,1);
```

FEATURE EXTRACTION OF EARTHQUAKE SIGNALS USING FRACTIONAL DOMAIN

```
plot(x1);  
    Subplot (3,1,2);  
plot(x2);  
subplot (3,1,3);  
plot (h1);
```

Output:

```
opsnr =1.0725.
```

Fractional Order:

```
clc;  
clearall;  
closeall;  
load'earth.txt'  
time=1:1:60000;  
x1=earth(:,3)';  
noise=(sin(2.*pi.*5500.*time./100));  
x2=x1+noise;  
    b=[2.407, 113.1,2808.0,36728.1,126390.2];  
    a=[48598.4];  
    y1=filter (b, a, x1);  
opsnr=((abs(y1.*y1))/(abs((y1-x2).*(y1-x2))))  
subplot (3,1,1);  
plot(x1);  
subplot (3,1,2);
```

FEATURE EXTRACTION OF EARTHQUAKE SIGNALS USING FRACTIONAL DOMAIN

```
plot(x2);  
subplot (3,1,3);  
plot (y1);
```

Output:

```
opsnr = 1.9988.
```

CONCLUSION:

It is concluded that the new featured Butterworth filter gives better lower order for given specification than the existing filter .It is also gives better spectral characteristics than existing Butterworth window that too better than the Dirichlett ,Triangle window functions.

Also the Signal to Noise Ratio which is calculated earlier is increased than usual, when compared between Conventional Butterworth Filter, Modified Butterworth Filter and Fractional Modified Butterworth Filter as mentioned in the previous chapter.

Thus our project successfully explains that the order of the filter gets reduced and the use of our Novel Butterworth Filter in the analysis of Earthquake Signals. The future scope of this project can be implemented using the FIR window techniques and predicting the Earthquake signals.

REFERENCES:

- [1] P.V. Muralidhar, “Feature extraction and pattern recognition earth quake signals using fractional domains”.
- [2] <https://en.wikipedia.org/wiki/Earthquake>.
- [3] F. J. Harris, “On the use of windows for harmonic analysis with the discrete Fourier transform,” Proc. IEEE, vol. 66, no. 1, pp. 51–83, Jan. 1978.
- [4] S. Kay and S. Marple, “Spectrum analysis-a modern perspective,” Proc. IEEE, vol. 69, no. 11, pp. 1380–1419, Nov. 1981.
- [5] M. H. Hayes, Statistical Signal Processing and Modeling. New York: Wiley, 1996.
- [6] P.V. Muralidhar, “A New Butterworth Featured Filter, Window Function, Differentiator and Integrator for Signal and Image Processing”.
- [7] N. Geckinli and D. Yavuz, “Some novel windows and a concise tutorial comparison of window families,” IEEE Trans. Acous. Speech Signal Processing, vol. ASSP-26, no. 6, pp. 501–507, Dec. 1978.
- [8] S. Mitra and J. Kaiser, Handbook for Digital Signal Processing. New York: Wiley, 1993.
- [9] B. P. Lathi, Modern Digital and Analog Communication Systems, 3rd ed., New York: Oxford Univ. Press, 1998.
- [10] Earthquake Analysis and Samples are explained by PulkitVelan, Student of M.S, IIIT-Hyderabad.
- [11] T. Yoon and E. Joo, “Butterworth window for power spectral density estimation,” ETRI J., vol. 31, no. 3, pp. 292–297, June 2009.
- [12] S. Mitra and J. Kaiser, Handbook for Digital Signal Processing. New York: Wiley, 1993.
- [13] P. Ramesh Babu, “Digital Signal Processing”, 4th edition, SCITECH publications (INDIA) pvt.ltd.
- [14] A. Acharya, S. Das, I. Pan, Sh. Das, “Extending the Concept of Analog Butterworth Filter for Fractional Order Systems”.
- [15] YangQuan Chen, Ivo Petras, and DingyuXue, “Fractional order control-a tutorial”, American Control Conference, ACC '09, pp. 1397-1411, June 2009, St. Louis, MO.

A New Butterworth Featured Filter, Window Function, Differentiator and Integrator for Signal and Image Processing

P.V. MURALIDHAR
AITAM, Tekkali (A.P) INDIA

Abstract

The Butterworth filter achieve its flatness at the expense of a relatively wide transition region from pass band to stop band with average transient characteristics. This filter is completely defined mathematically by two parameters i.e., cut-off frequency and the number of poles. In this proposal an attempt is made to derive new mathematical transfer function of Butterworth and which will compared with existing function in terms of order and its filter characteristics. Using the features of this new Butterworth transfer function, it is extended to use as a window function for spectral characteristics , implementation of differentiator and integrators and finally apply 2-D form low pass ,high pass filters for image enhancement.

Indexterms: Butterworth, window function, Differentiator and Integrator

1. Introduction

Digital signal processing (DSP) [1,2] technology plays an important role in modern society. The fundamental concept of DSP technology is done through important sub tools sub tasks like capturing and analog input signals, analog to digital conversion, filtering, and processing data and finally digital to analog conversion etc.,. Initial stage of processing usually sensors, are used to convert electrical to non-electrical signals. In this context window functions, differentiators and integrators are plays an important role to extract signals from preceeding to the succeeding stages and another important sub processing unit is filtering. The function of the filtering unit is significantly attenuate aliasing distortion. DS processors then, accepts the signals and process the data according to DSP rules such as band pass, high pass, low pass filtering or other algorithm for that different applications.

J.Harris[3] presented comprehensive catalog of data windows along with significant performance parameters like, bandwidth (BW), side lobe attenuation (SLA), ripple ratio etc., from which different window functions like Rectangular Bartlett, Hanning, Hamming etc., are analyzed. P.V.Muralidhar postulates on complete generalization of all window function in[4,5].

Most important parameters in spectral analysis of window functions are 3db B.W or HMLW and (SLA) or maximum side lobe level (MSLL). Windows can be categorized in to two types. They are fixed and variable windows. In fixed window, one parameter is to control bandwidth where as in second type, two or more parameters to control B.W and SLA [6-9].

Transfer function of Butterworth filter is used as a window[10] by considering a portion of impulse response, called as Butterworth window. This assumption considers cut-off frequency of the filter i.e., 3db bandwidth as the width of the window. The obtained spectral analysis of Butterworth window by applying Fourier transform to Butterworth filter. Butterworth windows are used as noise in reconstructed image and can also be used to remove edge effect of filter output in pattern matching algorithm.

Another important signal processing unit in DSP technology is differentiator and integrator. The design method of digital differentiator generally classified into two categories one is Finite

Impulse Response (FIR) and the other is Infinite Impulse Response (IIR) filter methods. In FIR the filter coefficients, are determined by Eigen filter method, window method, and limit computation method. In IIR the filter coefficients, are obtained from numerical integration rules.

Hence in this proposals an attempt is made to derive a novel mathematical transfer function of Butterworth and which will be compared with existing Butterworth in terms of order and filter characteristics. It is extended to use as window function to analyse the spectral characteristics of signal. And also presents FIR differentiator and integrator by using novel window function. It also extended to implement image enhancement by using novel Butterworth filter.

2. Proposed Butter Worth IIR Filter

In this paper main objective is to form a novel IIR filter equation.

The proposed mathematical formula is given by

$$H(j\Omega) = \frac{1}{\sqrt{\left(1 + \left(\frac{\exp\left(\frac{\Omega}{2.71828}\right)}{\Omega\rho}\right)^2\right)^{2N}}$$

- The formation for the conventional filter at the cut-off frequency($\Omega=\Omega_c$),The magnitude becomes 0.707 of its equivalent value and steady state error is zero at $\Omega=\infty$.
- Normally we calculating the transfer function with different mathematical function like cosine, sine, tan, log and finally exponential.
- But this transfer function gives the best results compared with other mathematical functions.
- For the standard specifications we get lower order compared with the existed butter worth filter.

$$N \geq \frac{\log\sqrt{\frac{\lambda}{\epsilon}}}{\log\left(\frac{\exp\left(\frac{\Omega}{2.71828}\right)}{\Omega\rho}\right)}$$

where $\lambda = \sqrt{(10^{0.1\alpha_s} - 1)}$

$\epsilon = \sqrt{(10^{0.1\alpha_p} - 1)}$

α_p = pass band attenuation

α_s = stop band attenuation

$\Omega\rho$ = pass band frequency

Ω_s = stop band frequency

Problemstatement: Given specification $\alpha_p=1\text{dB}$, $\alpha_s=30\text{dB}$; $\Omega_\rho = 200 \text{ rad/s}$; $\Omega_s=600 \text{ rad/sec}$;

determine N=?

Ans:

$$\sqrt{\frac{\lambda}{\epsilon}} = \sqrt{\frac{10^{0.1\alpha_s} - 1}{10^{0.1\alpha_p} - 1}} = \sqrt{\frac{10^3 - 1}{10^{0.1} - 1}} = 62.115$$

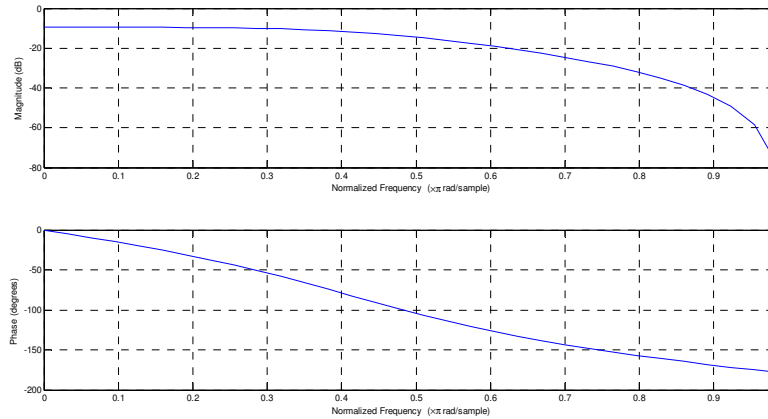
$$\frac{\Omega_s}{\Omega_\rho} = 3, \exp\left(\frac{\Omega_s}{\Omega_\rho}\right) = 7.3905$$

$$\frac{\Omega_s}{\Omega_\rho} = \frac{\log\sqrt{111}}{\log(7.3905)} = 1.177$$

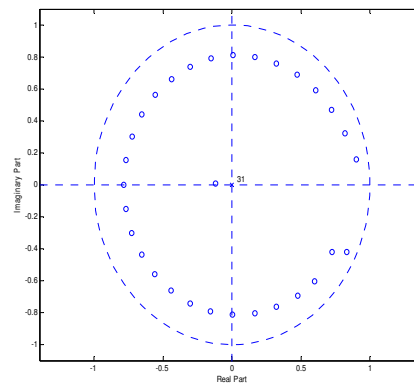
$$N = 2$$

For the same specifications existing Butterworth filter order is becomes '3'.

The figure2.1 shows the IIR filter responses.

Figure 2.1: Frequency response of an IIR filter(novel Butterwoth)

The following figure2.2 shows the z-plane of the IIR filter. The all poles are placed inside of the unit plane. So the system is stable.

Figure 2.2: Stability in z-plane**Table 2.1:** comparison of Butterworth & Novel Butterworth filter

Butter worth filter	Novel Butter worth filter
<ul style="list-style-type: none"> The Butter worth filter equation is given by, $H(j\Omega) = \frac{1}{\sqrt{\left(1 + \left(\frac{\Omega}{\Omega_c}\right)^2\right)^{2N}}}$ Where Ω = variable frequency, Ω_c=cut-off frequency, N= order. For specific order. Flat response in pass band Cut-off frequencies are easily find out due to flat response. No ripples in transition band 	<ul style="list-style-type: none"> The Novel Butter worth filter equation is given by, $H(j\Omega) = \frac{1}{\sqrt{\left(1 + \left(\frac{\exp\left(\frac{\Omega}{2.71828}\right)}{\Omega_c}\right)^2\right)^{2N}}}$ Where Ω = variable frequency, Ω_c=cut-off frequency, N= order. Order decreases. More flat response compared to butter worth Cut-off frequencies are accurately find out due to more flat response. No ripples in transition band

3. Novel Windowfunction

Here the novel butter worth filter transfer function is used as a novel butter worth window function.

The formula is given by,

$$\text{New Butterworth window}(w) = H(j\Omega) = \frac{1}{\sqrt{\left(1 + \left(\frac{\exp\left(\frac{k_1}{k_2}\right)}{2.71828}\right)^2\right)^{2N}}}$$

Where k_1 is variable frequency,
 k_2 is cut-off frequency and
 N is the order of the filter.

- In this window analysis the spectral parameters are controlled by cut-off frequency and order
- But where as in conventional windows no controlled parameters to analyze the spectral paramet
- The following table is the frequency characteristics of novel butterworth filter

Table 3.1: Frequency characteristics of novel butter worth filter

ORDER (N)	CUT OFF FREQUENCIES	BUTTERWORTH WINDOW (SIDE LOBE ATTENUATION)	NOVEL WINDOW FUNCTION (SIDE LOBE ATTENUATION)
2	0.3 π	-19.8dB	-27.5dB
2	0.4 π	-18.3dB	-18.1dB
3	0.5 π	-18.9dB	-18.7dB
3	0.4 π	-19.2dB	-18.5dB
4	0.5 π	-18.5dB	-18.1dB
4	0.6 π	-19dB	-18.4dB
5	0.5 π	-17.8dB	-17.4dB
5	0.6 π	-18.3dB	-17.7dB

The spectral characteristics of novel butterworth filter at different cut-off frequencies and different orders. Figure 3/2(a) to Figure 3.2(h)

Figure 3.2(a): Spectral characteristics of novel window function. $N=2$ $w_c=0.3\pi$

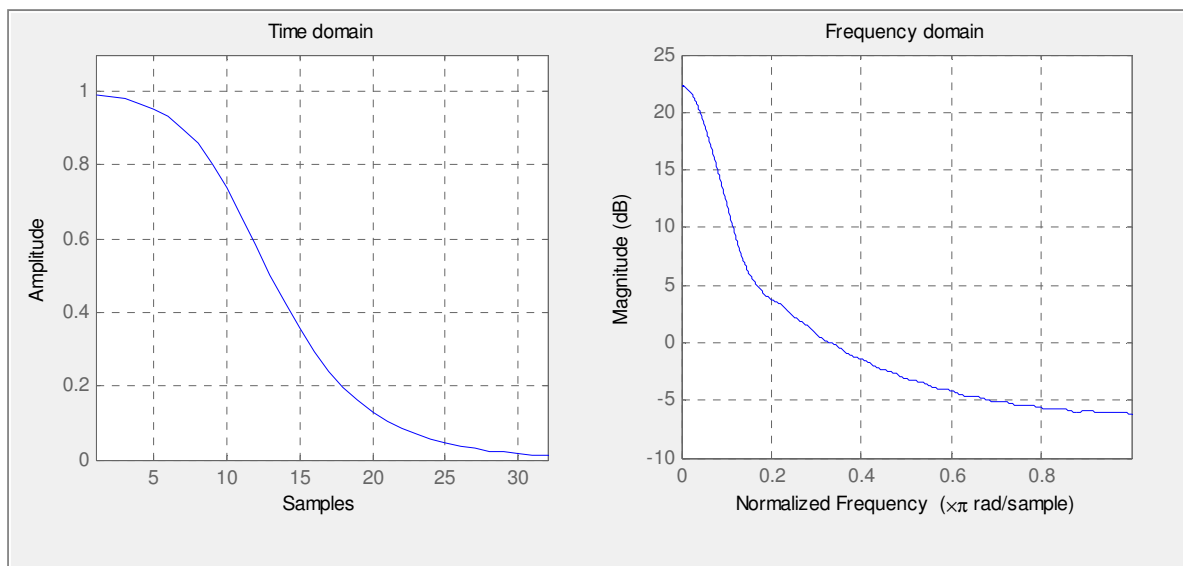


Figure 3.2(b): Spectral characteristics of novel window function. $N=2$ $w_c=0.4$ π

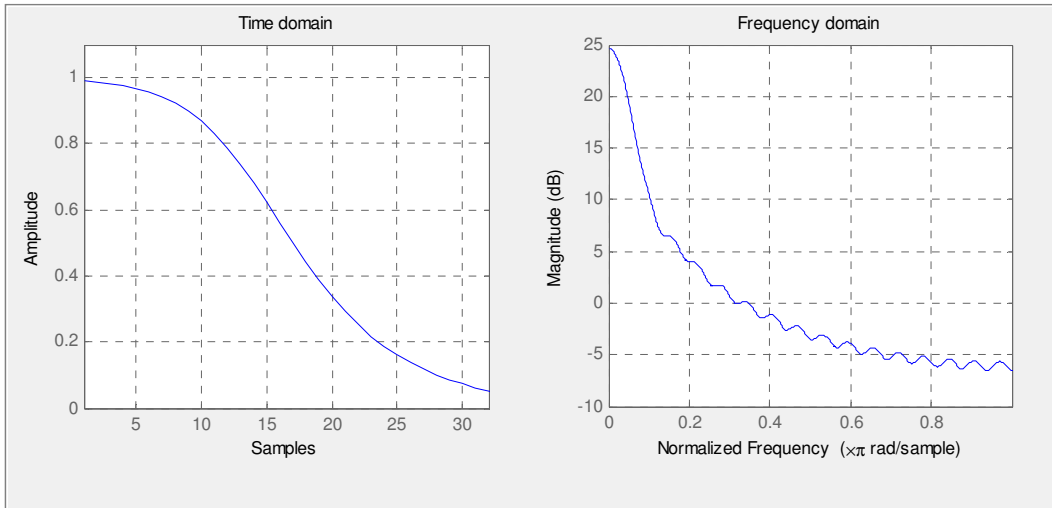


Figure 3.2(c): Spectral characteristics of novel window function. $N=2$ $w_c=0.5$ π

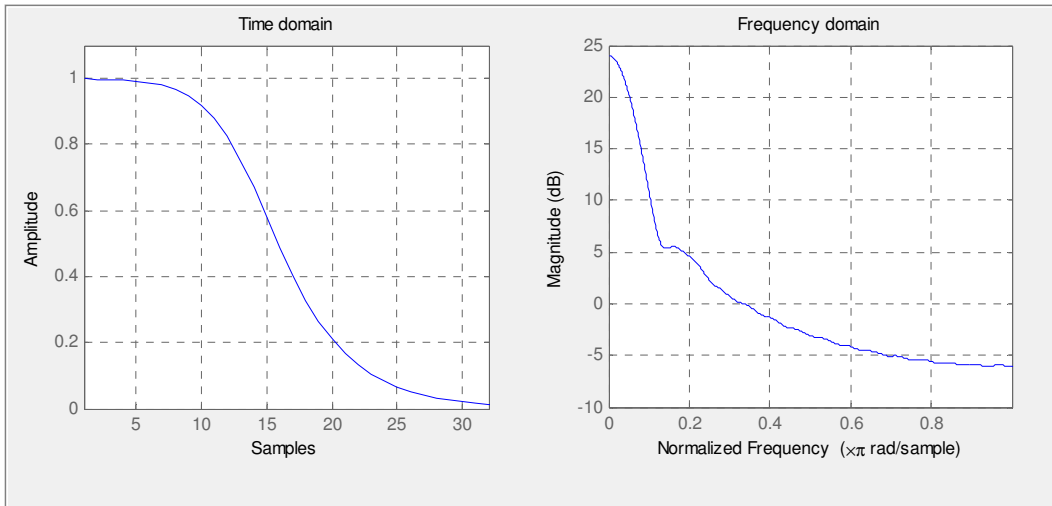


Figure 3.2(d): Spectral characteristics of novel window function. $N=2$ $w_c=0.6$ π

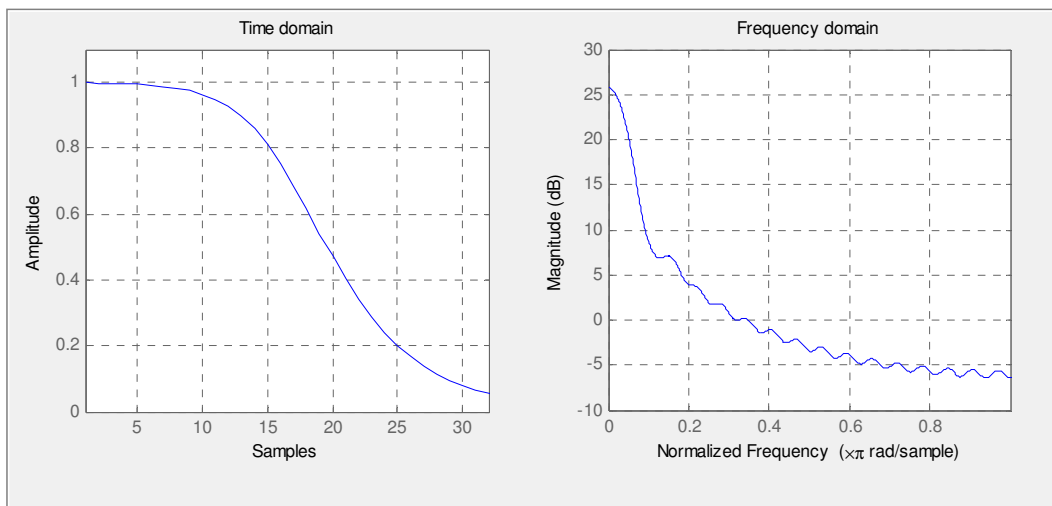


Figure 3.2(e): Spectral characteristics of novel window function. $N=4$ $w_c=0.5$ pi

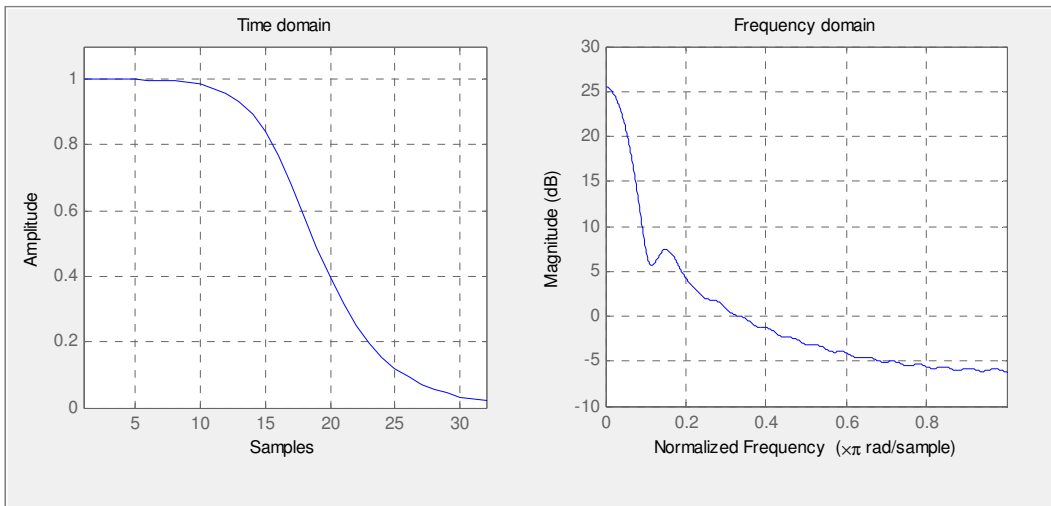


Figure 3.2(f): Spectral characteristics of novel window function. $N=4$ $w_c=0.6$ pi

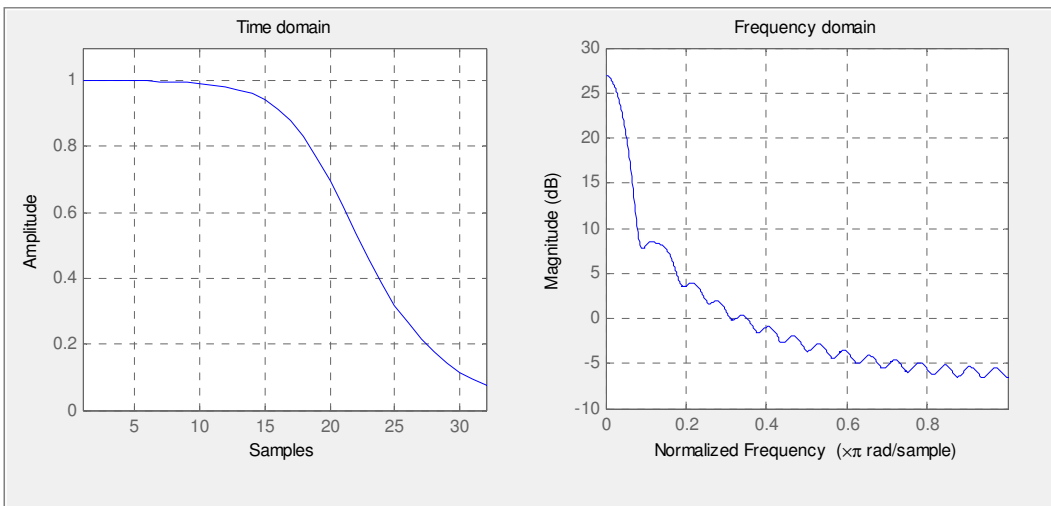


Figure 3.2(g): Spectral characteristics of novel window function. $N=4$, $w_c=0.5$ pi

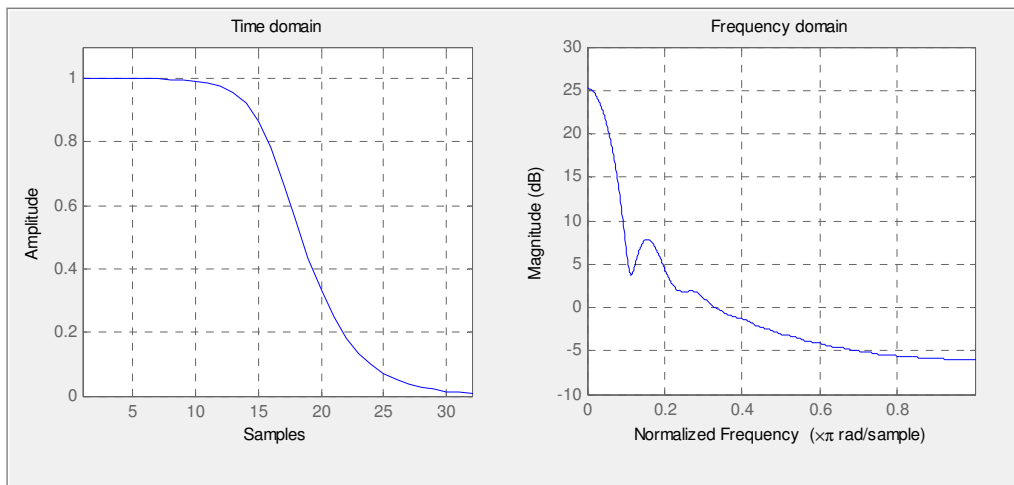
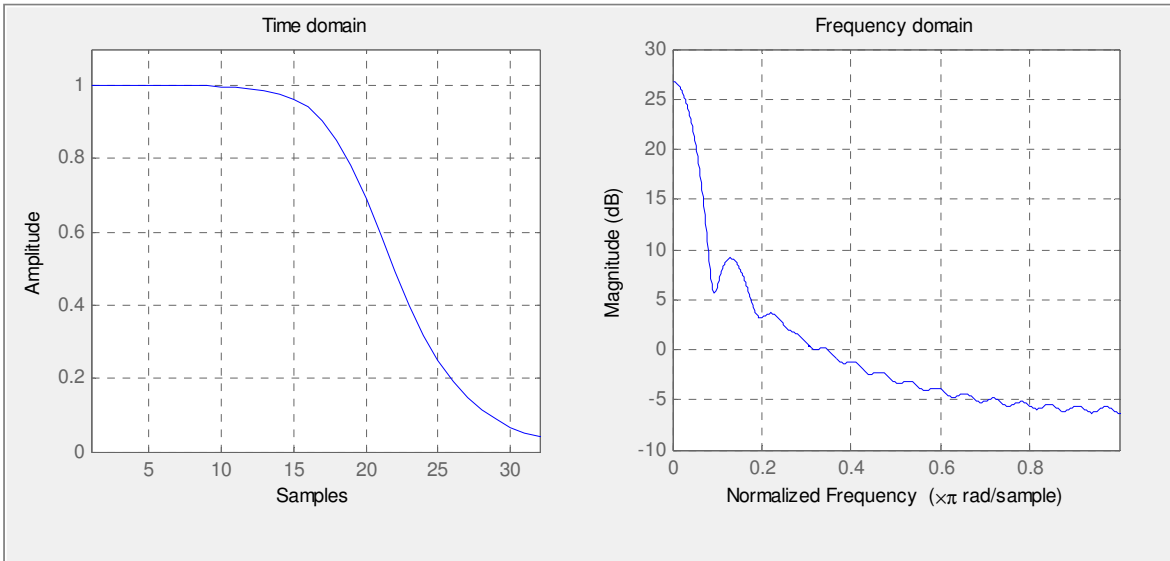


Figure 3.2(h): Spectral characteristics of novel window function. $N=5$ $w_c=0.6\pi$ **Table 3.2:** Comparison of frequency characteristics of different windows

WINDOW	3-dB BANDWIDTH	SIDE LOBE ATTENUATION
Rectangular	0.879 Hz	-13.3dB
Triangular	1.270 Hz	-26.5 dB
Butterworth ($f_c=0.439$ Hz)		
N=2	0.793 Hz	-18.2 dB
N=3	0.740 Hz	-24.3dB
N=4	0.731 Hz	-28.8 dB
Novel Butterworth ($f_c=0.439$ Hz)		
N =2	0.09375	-27.5dB
N=3	0.11719	-18.6dB
N=4	0.125	-18dB

The above table 3.2 shows the frequency characteristics of conventional window function, Butterworth window and novel Butterworth window function. The conventional windows are able to control 3-dB bandwidth or sidelobe attenuation by only one parameter in general. Thus, they cannot control these two characteristics independently. In other words, if we reduce a window function's 3-dB bandwidth, the sidelobe attenuation is also reduced, and vice versa. Butterworth window function that enables us to control both its 3-dB bandwidth (spectral resolution) and sidelobe attenuation (spectral leakage) independently. In this window analysis the spectral parameters are controlled by cut-off frequency and order.

4. Differentiator

The frequency response of an ideal digital differentiator is linearly proportional to frequency. It is given by

$$H_d(e^{j\omega}) = j\omega \quad \text{for } (-\pi \leq \omega \leq \pi)$$

The ideal impulse response of a digital differentiator with linear phase is given by

$$h_{d(n)} = \frac{1}{2\pi} \int_{-\pi}^{\pi} H_d(e^{j\omega}) e^{j\omega n} d\omega$$

$$= \frac{\cos \pi(n-\beta)}{n-\beta} - \frac{\sin(n-\beta)\pi}{\pi(n-\beta)^2}$$

Where, $\beta = \frac{N-1}{2}$.

If 'N' is odd, 'β' is an integer and we have $\sin(n - \beta) \pi = 0$ for any integer n. If 'N' is even, then $\cos \left[\frac{2n-(N-1)}{2} \pi \right] = 0$ for any integer.

Thus we have, for 'N' odd

$$h_d(n) = \frac{\cos[(n - \beta)\pi]}{n - \beta} \text{ for } n \neq \beta$$

$$= 0 \text{ for } n = \beta$$

And for 'N' even

$$h_d(n) = \frac{-\sin[(n - \beta)\pi]}{\pi(n - \beta)^2}$$

Both have the property $h_d = -h_d(N - 1 - n)$. The coefficients are asymmetric and of infinite length. The finite impulse response can be obtained by truncating them by using window of length N. The differentiator obtained by $h(\omega) = h_d(\omega) \cdot \omega(n)$

Where $\omega(n)$ = New window function

$h_d(\omega)$ = Impulse Infinite Response.

The waveforms of differentiator at different cut-off frequencies are given in from Figure 4.1 to Figure.4.3

Figure 4.1: Frequency and phase response of differentiator at $\omega_c=0.5$ [], $N=2$.

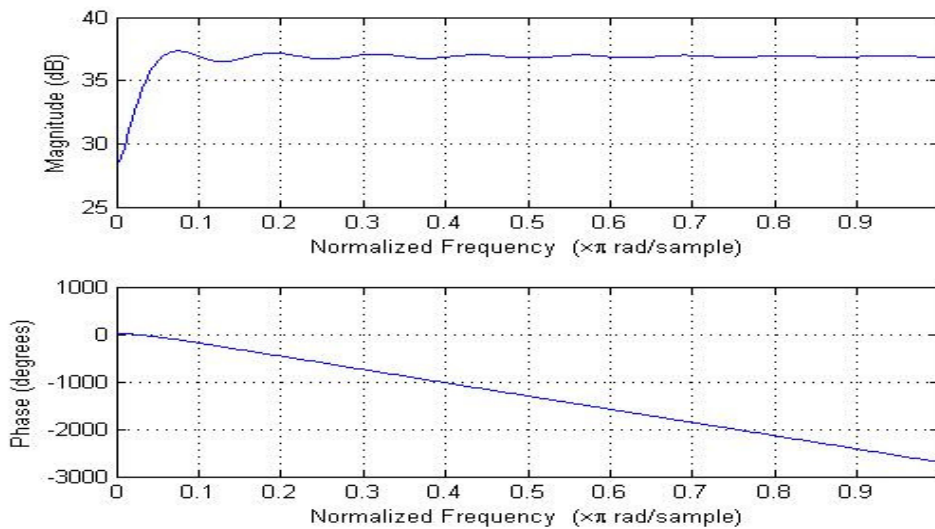
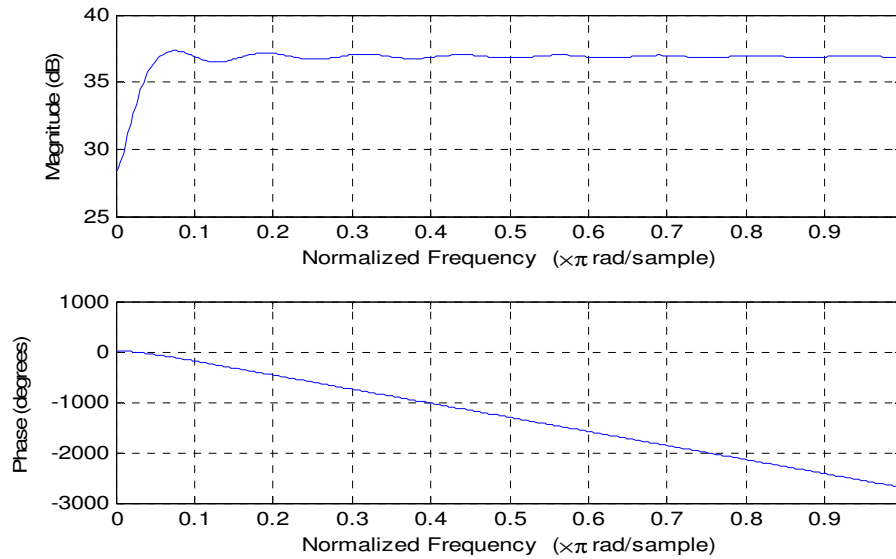
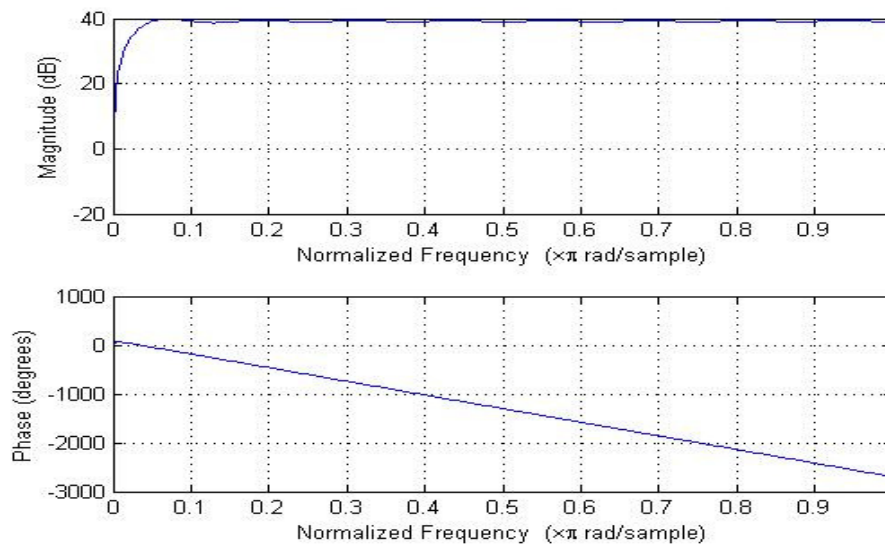


Figure 4.2: Frequency and phase response of differentiator at $\omega_c=0.7$ rad/sample, $N=2$.**Figure 4.3:** Frequency and phase response of differentiator at $\omega_c=0.9$ rad/sample, $N=2$.

5. Integrator

An integrator produces a steadily changing output voltage for a constant input voltage. Integrator is an important component for realizing various functions which may not be recognized by differentiator. Integrators and differentiators are inverse each other.

The waveforms of Integrator at different cut-off frequencies are given in from figure 5.1 to figure 5.2

Figure 5.1: Frequency and phase response of Integrator $w_c=0.5$, $N=2$.

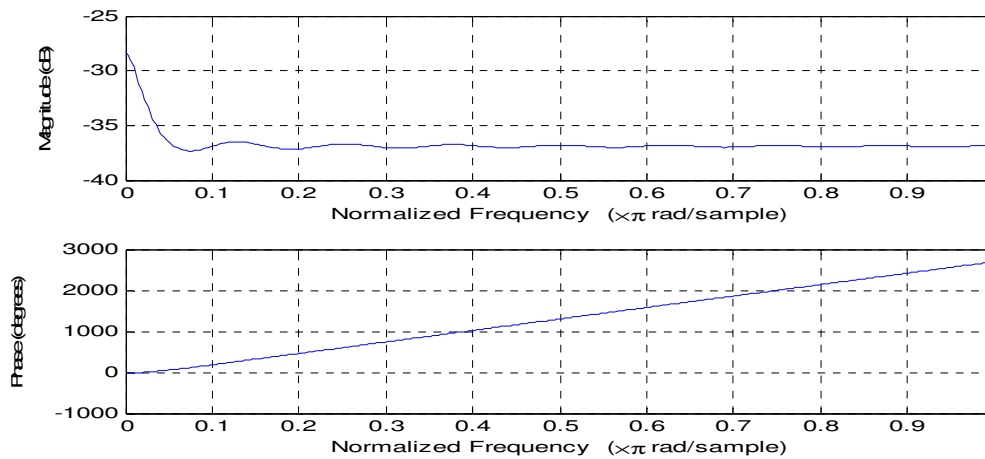
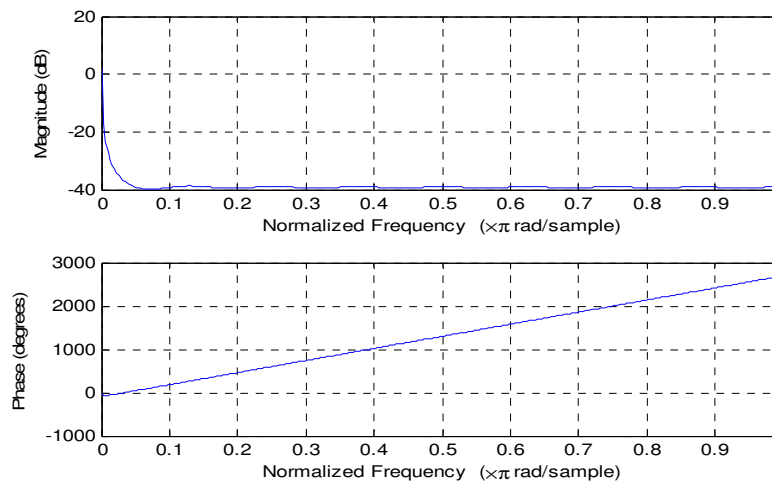


Figure 5.2: Frequency and phase response of Integrator $w_c=0.7$, $N=2$.



6. Image Enhancement

Image enhancement techniques are designed to improve the quality of an image as perceived by a human being. Image enhancement can be performed both in the spatial as well as in the frequency domain. The objective of image enhancement is to improve the interpretability of the information present in images for human viewers. An enhancement algorithm is one that yields a better-quality image for the purpose of some particular application which can be done by either suppressing the noise or increasing the image contrast. Image enhancement algorithms are employed to emphasize, sharpen image features for display and analysis. Enhancement methods are application specific and we often developed empirically. Image enhancement techniques emphasize specific image features to improve the visual perception of an image. Image enhancement techniques can be classified into two broad categories as

1. Spatial domain method.
2. Frequency domain method.

The spatial domain method operates directly on pixels, whereas the frequency domain method operates on the Fourier transform of an image and then it back to the spatial domain. Elementary enhancement techniques are histogram based because they are simple, fast, and with them acceptable

results for some applications can be achieved. Unsharp masking sharpens the edges by subtracting a portion of a filtered component from the original image. The technique of unsharp masking has become a popular enhancement tool to assist in diagnosis.

6.1 Frequency Domain Methods

- The concept of filtering is easier to visualize in the frequency domain. Therefore, enhancement of image $f(m,n)$ can be done in the frequency domain, based on its DFT

$F(u, v)$.

- This is particularly useful; if the spatial extent of the point spread sequence $h(m, n)$ is large. In this case, the convolution may be computationally unattractive.

$$g(m, n) = h(m, n) * f(m, n)$$

Where $g(m, n)$ is the enhanced image,

$h(m, n)$ is the point spread function,

$f(m, n)$ is the given image.

- We can therefore directly design a transfer function $H(u, v)$ and implement the enhancement in the frequency domain as follows:

$$G(u, v) = H(u, v)F(u, v)$$

Where $G(u, v)$ is the enhanced image,

$H(u, v)$ is the Transfer function,

And $F(u, v)$ is the given image.

6.1.1 Lowpass Filtering

- Edges and sharp transitions in gray values in an image contribute significantly to high-frequency content of its Fourier transform.
- Regions of relatively uniform gray values in an image contribute to low-frequency content of its Fourier transform.
- Hence, an image can be smoothed in the Frequency domain by attenuating the high-frequency content of its Fourier transform. This would be a lowpass filter
- For simplicity, we will consider only those filters that are real and radials symmetric.

6.1.1.1 Butterworth Low Pass Filter

- A two-dimensional Butterworth lowpass filter has transfer function:

$$H(u, v) = \frac{1}{1 + \left[\frac{\sqrt{u^2 + v^2}}{r_0} \right]^{2n}}$$

- n : filter order, r_0 : cutoff frequency.
- Frequency response does not have a sharp transition as in the ideal LPF.
- This is more appropriate for image smoothing than the ideal LPF, since this not introduce ringing.
- Frequency response does not have a sharp transition as in the ideal LPF.

The output images of butter worth low pass filter at different cut-off frequencies are given below figure 6.1(a) to figure 6.1(d)

6.1.1.2 Butterworth High Pass Filter

Edges and sharp transitions in grayvalues in an image contribute significantly to high-frequency content of its Fourier transform. Regions of relatively uniform gray values in an image contribute to low-frequency content of its Fourier transform. Hence, image sharpening in the Frequency domain can be done by attenuating the low-frequency content of its Fourier transform. This would be a high pass filter. For simplicity, we will consider only those filters that are real and radials symmetric. The output

images of butter worth high pass filter at different cut-off frequencies are given below figure 6.1.1.2(a) to figure 6.1.1.2(d)

6.2 PEAK SIGNAL TO NOISE RATIO:

The term **peak signal-to-noise ratio (PSNR)** is an expression for the ratio between the maximum possible value (power) of a signal and the power of distorting noise that affects the quality of its representation. Because many signals have a very wide **dynamic range**, (ratio between the largest and smallest possible values of a changeable quantity) the **PSNR** is usually expressed in terms of the logarithmic decibel scale.

Image enhancement or improving the visual quality of a digital image can be subjective. Saying that one method provides a better quality image could vary from person to person. For this reason, it is necessary to establish quantitative/empirical measures to compare the effects of image enhancement algorithms on image quality.

Using the same set of tests images, different image enhancement algorithms can be compared systematically to identify whether a particular algorithm produces better results. The metric under investigation is the **peak-signal-to-noise ratio**. If we can show that an algorithm or set of algorithms can enhance a degraded known image to more closely resemble the original, then we can more accurately conclude that it is a better algorithm.

The PSNR is most commonly used as a measure of quality of reconstruction of lossy compression codes (e.g., for image compression). The signal in this is the original data, and the noise is the error introduced by compression. When comparing compression codes it is used as an approximation to human perception of reconstruction quality, therefore in some cases one reconstruction may appear to be closer to the original than another, even though it has a lower PSNR (a higher PSNR would normally indicate that the reconstruction is of higher quality).

For the following implementation, let us assume we are dealing with a standard 2D array of data or matrix. The dimensions of the correct image matrix and the dimensions of the degraded image matrix must be identical.

The mathematical representation of the **PSNR** is as follows:

$$PSNR = 20 \log_{10} \left(\frac{MAX_f}{\sqrt{MSE}} \right)$$

Where the **MSE** (Mean Squared Error) is:

$$MSE = \frac{1}{mn} \sum_0^{m-1} \sum_0^{n-1} \|f(i,j) - g(i,j)\|^2$$

It is most easily defined via the mean squared error (MSE) which for two m x n monochrome images f and g where one of the images is considered a noisy approximation of the other is defined as above.

Here, MAX_f is the maximum possible pixel value of the image. When the pixels are represented using 8 bits per sample, this is 255. More generally, when samples are represented using linear PCM with B bits per sample, MAX_f is $2^B - 1$. For colour images with three RGB values per pixel, the definition of PSNR is the same except the MSE is the sum over all squared value differences divided by image size and by three.

This can also be represented in a text based format as:

$$MSE = (1/(m*n))*sum(sum((f-g).^2))$$

$$PSNR = 20*log(max(max(f)))/((MSE)^0.5)$$

Modified Butter worth filter-2

The modified Butter worth filter -2 equation is given by,

$$H(j\Omega) = \frac{1}{\sqrt{\left(1 + \left(\frac{\tan\left(\frac{\Omega}{\Omega_c}\right)}{1.5574}\right)^2\right)^{2N}}}$$

Where Ω = variable frequency,

Ω_c =cut-off frequency,

N=order

A complete analysis of image enhancement using Butterworth, new Butterworth and Modified butter worth filter is given in from figure 6.2.1 to figure 6.2.3.for low –pass filter and from figure 6.2.4 to figure 6.2.6 for high-pass filter.(Observe from Tables 6.1 and table 6.2)

Table 6.1: PSNR values of Low Pass filters

S.NO.	ORDER	CUT-OFF FREQUENCY (Hz.,)	EXISTED BUTTER WORTH FILTER PSNR VALUE (dB,)	New BUTTER WORTH FILTER PSNR VALUE (dB,)	MODIFIED BUTTER WORTH FILTER PSNR VALUE (dB,)
1	8	1000	43.8640	44.1947	31.3021
2	8	100	36.7965	36.1121	36.0671
3	2	100	37.6921	34.6619	36.3839
4	1	0.5	25.3617	25.3918	25.2335
5	1	0.4	25.1577	25.1944	25.1780

Table 6.2: PSNR values of High Pass Filters

S.NO.	ORDER	CUT-OFF FREQUENCY (Hz.,)	EXISTED BUTTER WORTH FILTER PSNR VALUE (dB,)	NOVEL BUTTER WORTH FILTER PSNR VALUE (dB,)	MODIFIED BUTTER WORTH 2 FILTER PSNR VALUE (dB,)
1	8	1000	24.3678	24.4083	24.4082
2	8	100	24.5182	24.5571	24.4083
3	2	100	24.4738	24.5162	24.4063
4	1	100	24.4590	24.5025	24.4075
5	4	100	24.4969	24.5352	24.4101

Figure 6.2.1 (a,b,c): Low-pass Filter for image in frequency domain Butterworth Low-pass filter at cut-off frequency(f_c)=1000 & order(N)=8,

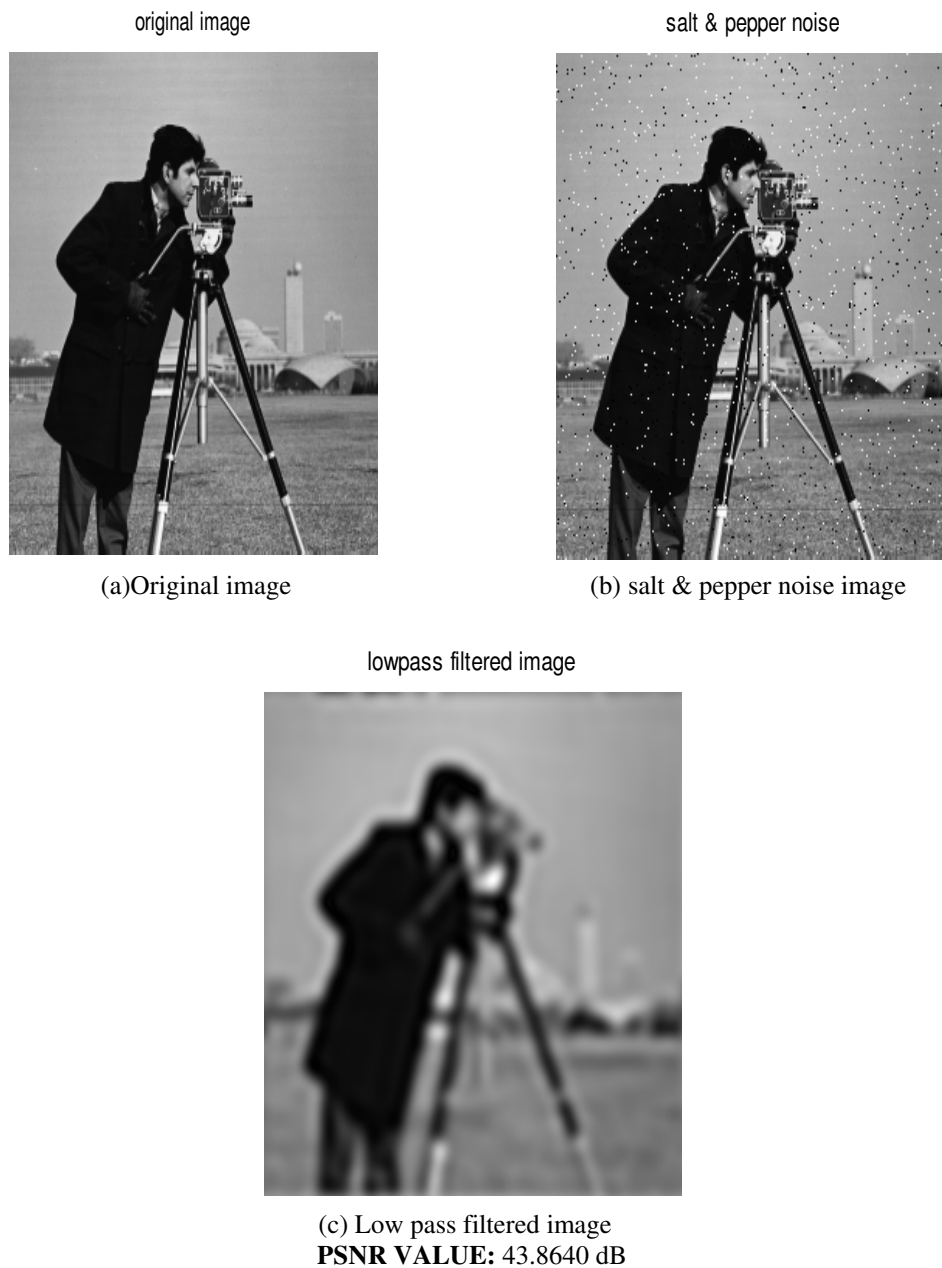


Figure 6.2.2 (a,b,c): Low-pass Filter for image in frequency domain new Butterworth Low-pass filter at cut-off frequency(f_c)=1000 & order(N)=8,

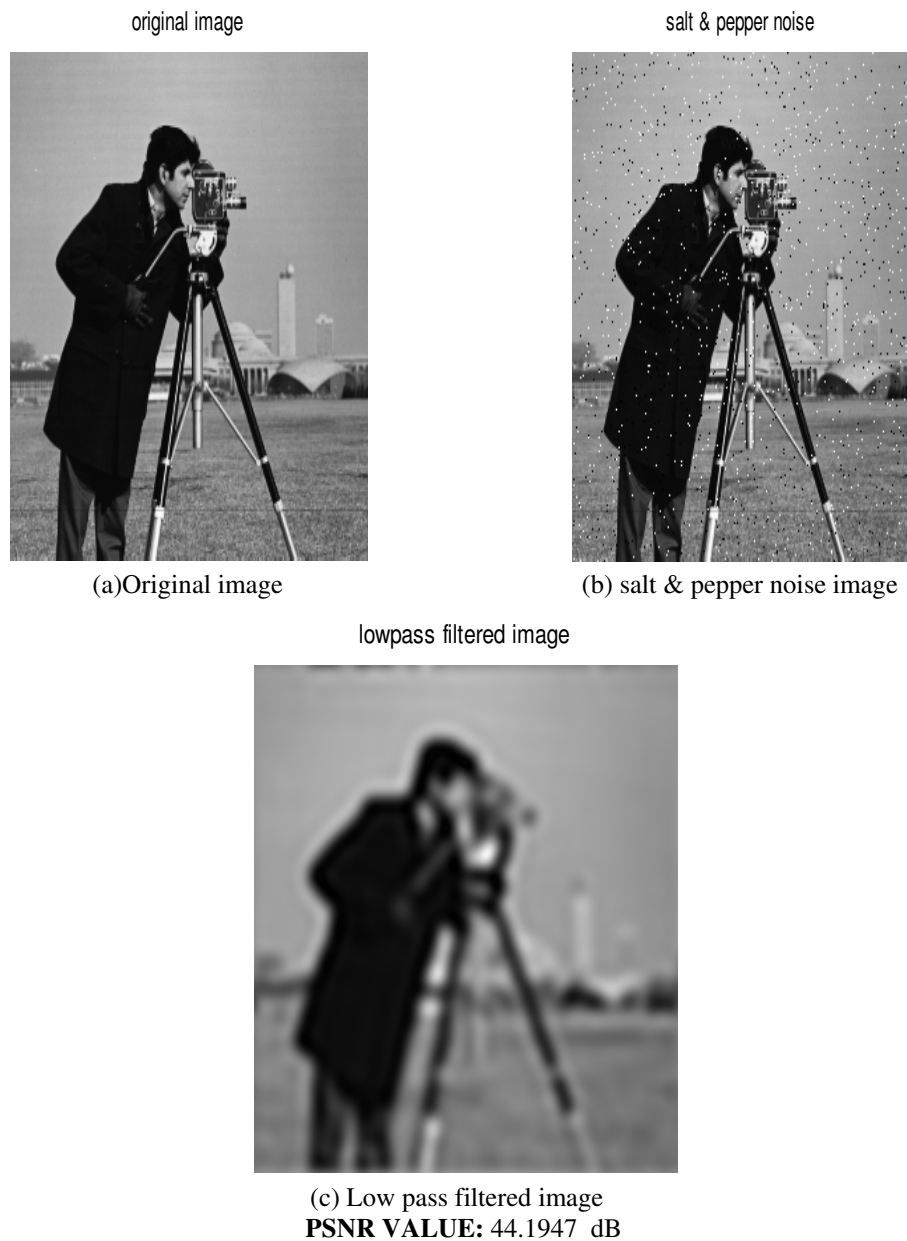


Figure 6.2.3 (a,b,c): Low-pass Filter for image in frequency domain modified Butterworth Low-pass filter at cut-off frequency $(f_c)=1000$ & order $(N)=8$,

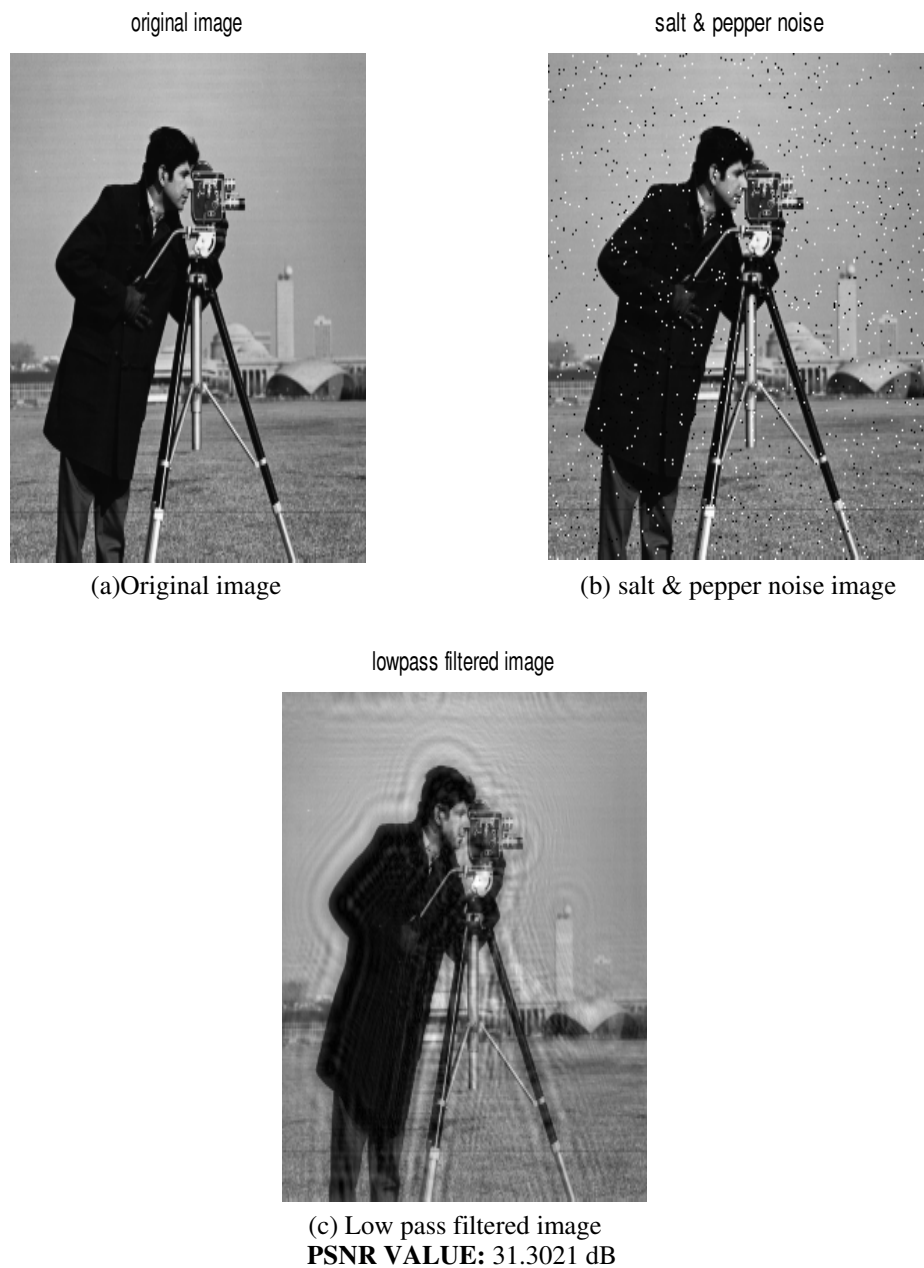


Figure 6.2.4 (a,b,c): High-pass Filter for image in frequency domain Butterworth Low-pass filter at cut-off frequency(f_c)=1000 & order(N)=8,

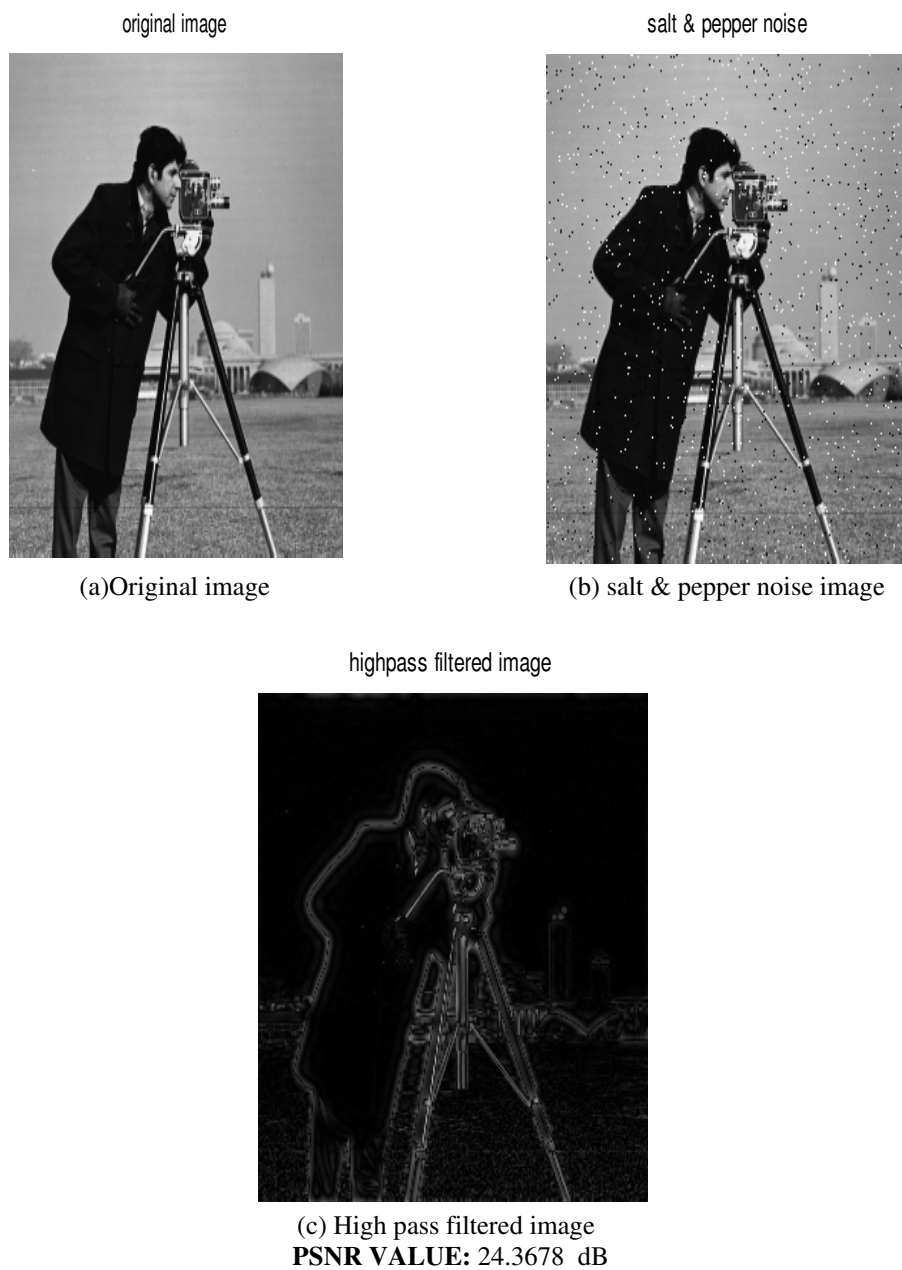


Figure 6.2.5 (a,b,c): High-pass Filter for image in frequency domain new Butterworth Low-pass filterat cut-off frequency(f_c)=1000 &order(N)=8,

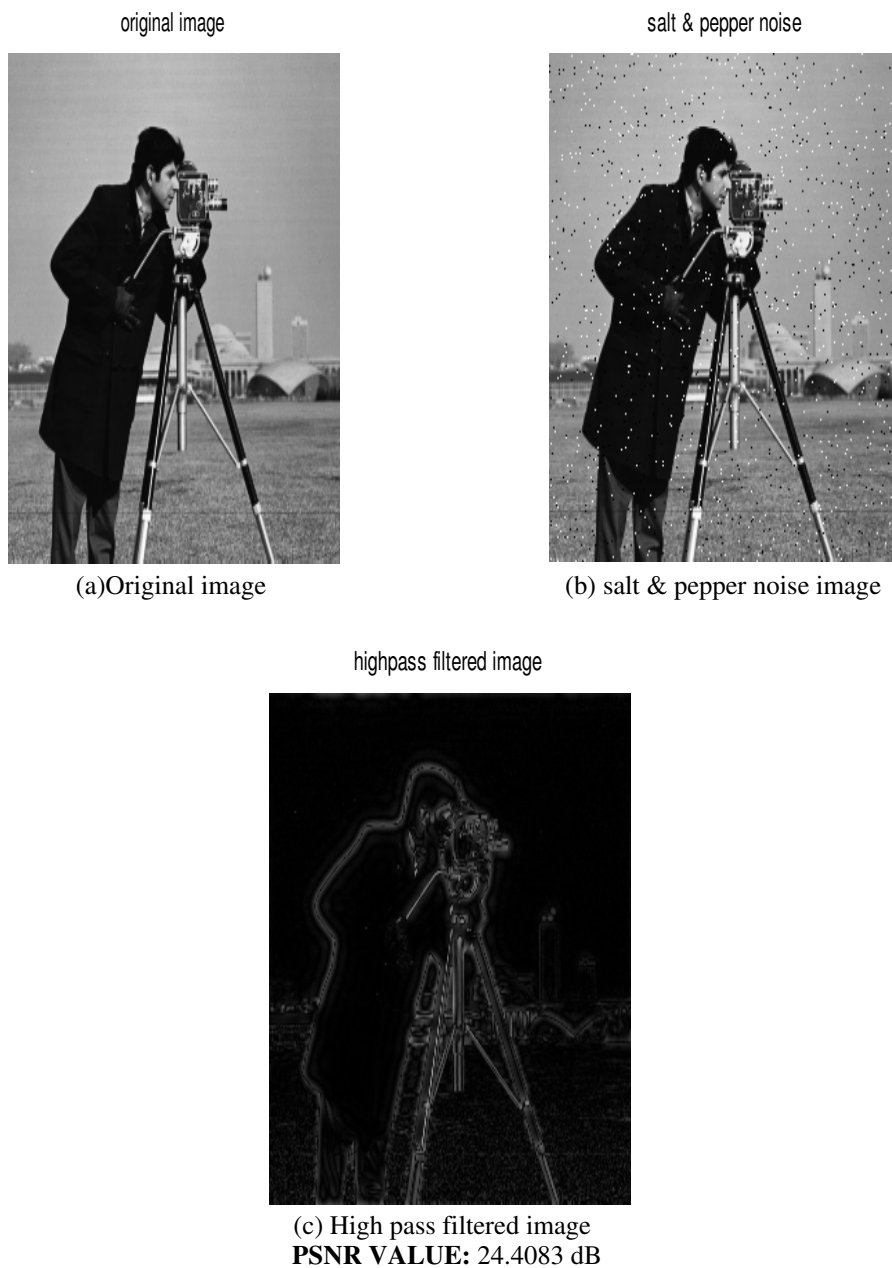
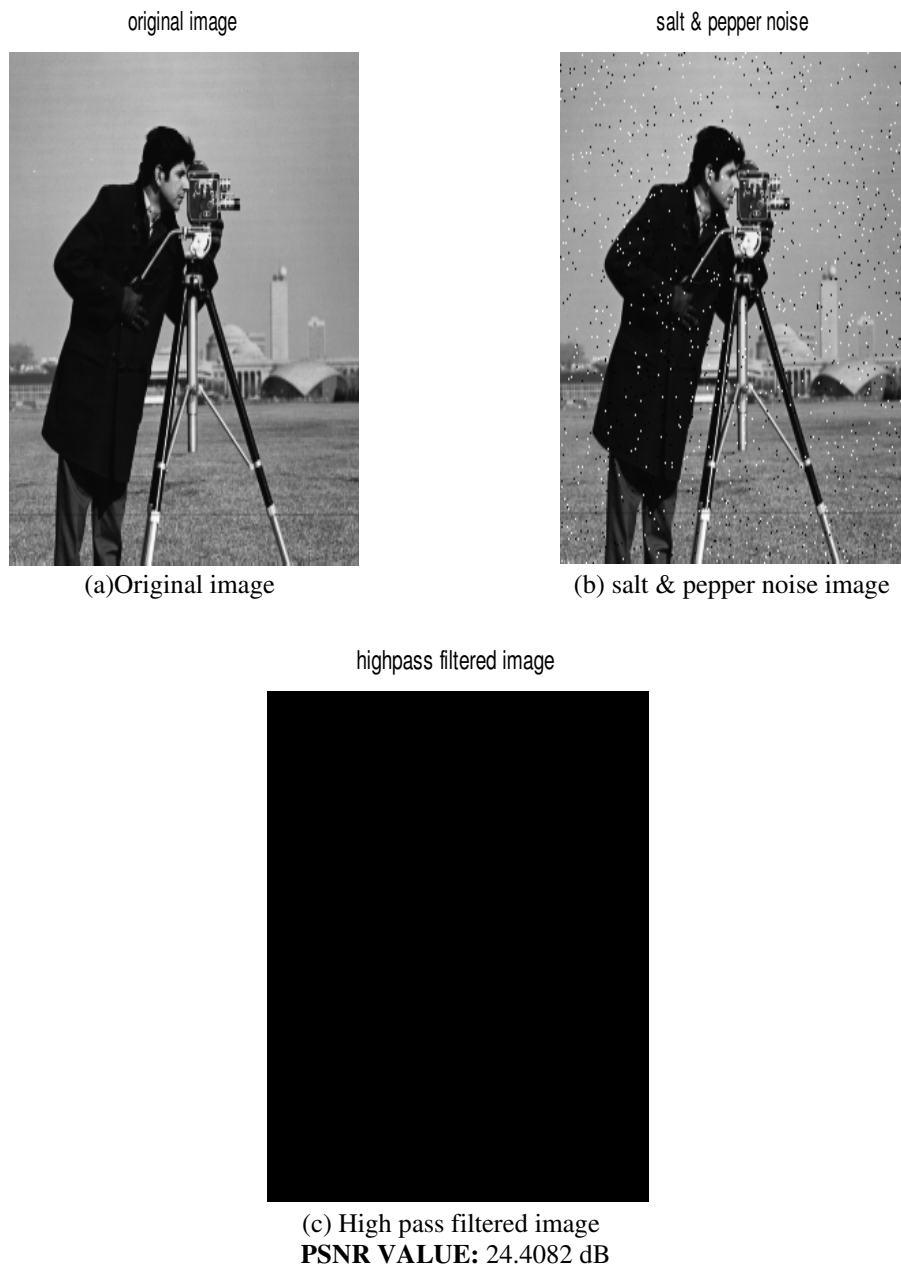


Figure 6.2.6 (a,b,c): High-pass Filter for image in frequency domain modified Butterworth Low-pass filter at cut-off frequency(f_c)=1000 & order(N)=8,



Conclusion

It is concluded that the new featured Butterworth filter gives better lower order for given specification than the existing filter .It is also gives better spectral characteristics than existing Butterworth window that too better than the Dirichlett ,Triangle window functions.

Acknowledgment

I am very much thankful to University Grants Commission (UGC), INDIA. This work is partly supported for the project sanctioned to me proposal No.4-4/1 2014-15(MRP-SEM/UGC-SERO) 1074.

References

- [1] M. H. Hayes, Statistical Signal Processing and Modeling. New York: Wiley, 1996.
- [2] B. P. Lathi, Modern Digital and Analog Communication Systems, 3rd ed., New York: Oxford Univ. Press, 1998.
- [3] F. J. Harris, "On the use of windows for harmonic analysis with the discrete Fourier transform," Proc. IEEE, vol. 66, no. 1, pp. 51–83, Jan. 1978.
- [4] Muralidhar, P. V., et al. "Generalization of Windows using Discrete Fractional Fourier Transform." International Conference on Innovations in Engineering and Technology (ICIET'2013) Dec. 25-26, 2013 Bangkok (Thailand).
- [5] P.V.Muralidhar,S.K.Nayak."Generalization of fixed and flexible window function".vol.2,issue 3.,pgs:9-13, imanager's Journal on Digital Signal Processing (JDP).
- [6] S. Orfanidis, Introduction to Signal Processing. Englewood Cliffs, NJ: Prentice-Hall, 1996.
- [7] P.V.Muralidhar, D Nataraj, V Iokesh Raju, Sumanth K Naik,"Implementation of different FIR high pass filters using fractional Kaiser window" pp V2-651-V2-655 (ICSPS), 2010, IEEE xplore.
- [8] P.V.Muralidhar, VL Nsastry D, SK Nayak,"Interpretation of Dirichlet, Bartlett, Hanning and Hamming windows using Fractional Fourier Transform" - International Journal of Scientific & Engineering(ijser) 2013.
- [9] P.V.Muralidhar, AS Srinivasa Rao, SK Nayak."Spectral interpretation of sinusoidal wave using fractional Fourier transform based FIR window functions" - Int. Rev. Comput. Softw(irecos), 2009.
- [10] Tae Hyun Yoon and Eon KyeongJoo."A Flexible Window Function for Spectral Analysis".IEEE signal processing magazine [139] march 2010.